UNIVERSITY OF AMSTERDAM

UvA-DARE (Digital Academic Repository)

Observations of Low and Intermediate Spectral Peak Blazars with the Imaging X-Ray Polarimetry Explorer

Marshall, H.L.; Ng, C. -Y.; Vink, J.; IXPE

DOI
10.3847/1538-4357/ad5671

Publication date
2024

Document Version
Final published version

Published in
Astrophysical Journal

License
CC BY

Link to publication

Citation for published version (APA):
Marshall, H. L., Ng, C. .-Y., Vink, J., & IXPE (2024). Observations of Low and Intermediate Spectral Peak Blazars with the Imaging X-Ray Polarimetry Explorer. *Astrophysical Journal*, *972*(1), Article 74. https://doi.org/10.3847/1538-4357/ad5671

General rights
It is not permitted to download or to forward/distribute the text or part of it without the consent of the author(s) and/or copyright holder(s), other than for strictly personal, individual use, unless the work is under an open content license (like Creative Commons).

Disclaimer/Complaints regulations
If you believe that digital publication of certain material infringes any of your rights or (privacy) interests, please let the Library know, stating your reasons. In case of a legitimate complaint, the Library will make the material inaccessible and/or remove it from the website. Please Ask the Library: https://uba.uva.nl/en/contact, or a letter to: Library of the University of Amsterdam, Secretariat, P.O. Box 19185, 1000 GD Amsterdam, The Netherlands. You will be contacted as soon as possible.

UvA-DARE is a service provided by the library of the University of Amsterdam (https://dare.uva.nl)

Download date:13 Oct 2026

The Astrophysical Journal, 972:74 (19pp), 2024 September 1 https://doi.org/10.3847/1538-4357/ad5671
© 2024. The Author(s). Published by the American Astronomical Society.
OPEN ACCESS

Observations of Low and Intermediate Spectral Peak Blazars with the Imaging X-Ray Polarimetry Explorer

Herman L. Marshall[1], Ioannis Liodakis[2,3], Alan P. Marscher[4], Niccolò Di Lalla[5], Svetlana G. Jorstad[4,6], Dawoon E. Kim[7,8,9], Riccardo Middei[10,11], Michela Negro[12], Nicola Omodei[5], Abel L. Peirson[5], Matteo Perri[10,13], Simonetta Puccetti[10], Marco Laurenti[10], Iván Agudo[14], Giacomo Bonnoli[14,15], Andrei V. Berdyugin[16], Elisabetta Cavazzuti[17], Nicole Rodriguez Cavero[18], Immacolata Donnarumma[17], Laura Di Gesu[17], Jenni Jormanainen[16,19], Henric Krawczynski[18], Elina Lindfors[16,19], Greg Madjeski[20], Frédéric Marin[21], Francesco Massaro[22,23], Luigi Pacciani[7], Juri Poutanen[16], Fabrizio Tavecchio[15], Pouya M. Kouch[16,19], Francisco José Aceituno[14], Maria I. Bernardos[14], Víctor Casanova[14], Maya García-Comas[14], Beatriz Agís-González[3,14], César Husillos[14], Alessandro Marchini[24], Alfredo Sota[14], Dmitry Blinov[3,25], Ioakeim G. Bourbah[25], Sebastian Kielhmann[3,25], Evangelos Kontopodis[25], Nikos Mandarakas[25,26], Stylianos Romanopoulos[25,27], Raphael Skalidis[25,26], Anna Vervelaki[25], George A. Borman[28], Evgenia N. Kopatskaya[6], Elena G. Larionova[6], Daria A. Morozova[6], Sergey S. Savchenko[6,29,30], Andrey A. Vasilyev[6], Alexey V. Zhovtan[28], Carolina Casadio[25,26], Juan Escudero[31], Joana Kramer[32], Ioannis Myserlis[33,34], Efthalia Trainou[35], Ryo Imazawa[36], Mahito Sasada[37], Yasushi Fukazawa[36,38,39], Koji S. Kawabata[36,38,39], Makoto Uemura[36,38,39], Tsunefumi Mizuno[38], Tatsuya Nakaoka[38], Hiroshi Akitaya[40], Joseph R. Masiero[41], Dimitri Mawet[41], Georgia V. Panopoulou[41], Samaporn Tinyanont[42], Masato Kagitani[43], Vadim Kravtsov[16], Takeshi Sakanoi[43], Matthew Dattolo[44], Mark Gurwell[45], Garrett Keating[45], Ramprasad Rao[45], Whee Yeon Cheong[46,47], Hyeon-Woo Jeong[46,47], Sincheol Kang[46], Sang-Hyun Kim[46,47], Sang-Sung Lee[46,47], Emmanouil Angelakis[48], Alexander Kraus[34], Antonio Hales[49,50], Seiji Kameno[51,52], Ruediger Kneissl[53,54], Hugo Messias[49], Hiroshi Nagai[55,56], Lucio A. Antonelli[10,13], Matteo Bachetti[57], Luca Baldini[58,59], Wayne H. Baumgartner[2], Ronaldo Bellazzini[58], Stefano Bianchi[60], Stephen D. Bongiorno[2], Raffaella Bonino[22,61], Alessandro Brez[58], Niccolò Bucciantini[62,63,64], Fiamma Capitanio[7], Simone Castellano[58], Chen-Ting Chen[65], Stefano Ciprini[10,66], Enrico Costa[7], Alessandra De Rosa[7], Ettore Del Monte[7], Alessandro Di Marco[7], Victor Doroshenko[67], Michal Dovčiak[68], Steven R. Ehlert[2], Teruaki Enoto[69], Yuri Evangelista[7], Sergio Fabiani[7], Riccardo Ferrazzoli[7], Javier A. Garcia[41,70], Shuichi Gunji[71], Kiyoshi Hayashida[72], Jeremy Heyl[73], Wataru Iwakiri[74], Philip Kaaret[2], Vladimir Karas[68], Fabian Kislat[75], Takao Kitaguchi[69], Jeffery J. Kolodziejczak[2], Fabio La Monaca[7], Luca Latronico[22], Simone Maldera[22], Alberto Manfreda[58], Andrea Marinucci[17], Giorgio Matt[60], Ikuyuki Mitsuishi[76], Fabio Muleri[7], C.-Y. Ng[77], Stephen L. O'Dell[2], Chiara Oppedisano[22], Alessandro Papitto[13], George G. Pavlov[78], Melissa Pesce-Rollins[58], Pierre-Olivier Petrucci[79], Maura Pilia[57], Andrea Possenti[57], Brian D. Ramsey[2], John Rankin[7], Ajay Ratheesh[7], Oliver J. Roberts[65], Roger W. Romani[5], Carmelo Sgrò[58], Patrick Slane[45], Paolo Soffitta[7], Gloria Spandre[58], Douglas A. Swartz[65], Toru Tamagawa[69], Roberto Taverna[80], Yuzuru Tawara[76], Allyn F. Tennant[2], Nicholas E. Thomas[2], Francesco Tombesi[9,66,81], Alessio Trois[57], Sergey S. Tsygankov[16], Roberto Turolla[80,82], Jacco Vink[83], Martin C. Weisskopf[2], Kinwah Wu[82], Fei Xie[7,84], and Silvia Zane[82]

[1] MIT Kavli Institute for Astrophysics and Space Research, Massachusetts Institute of Technology, 77 Massachusetts Avenue, Cambridge, MA 02139, USA; hermanm@mit.edu
[2] NASA Marshall Space Flight Center, Huntsville, AL 35812, USA
[3] Institute of Astrophysics, Foundation for Research and Technology-Hellas, GR-70013 Heraklion, Greece
[4] Institute for Astrophysical Research, Boston University, 725 Commonwealth Avenue, Boston, MA 02215, USA
[5] Department of Physics and Kavli Institute for Particle Astrophysics and Cosmology, Stanford University, Stanford, CA 94305, USA
[6] Saint Petersburg State University, 7/9 Universitetskaya nab., 199034 St. Petersburg, Russia
[7] INAF Istituto di Astrofisica e Planetologia Spaziali, Via del Fosso del Cavaliere 100, 00133 Roma, Italy
[8] Dipartimento di Fisica, Università degli Studi di Roma "La Sapienza", Piazzale Aldo Moro 5, 00185 Roma, Italy
[9] Dipartimento di Fisica, Università degli Studi di Roma "Tor Vergata", Via della Ricerca Scientifica 1, 00133 Roma, Italy
[10] Space Science Data Center, Agenzia Spaziale Italiana, Via del Politecnico snc, 00133 Roma, Italy
[11] INAF Osservatorio Astronomico di Roma, Via Frascati 33, 00040 Monte Porzio Catone (RM), Italy
[12] Department of Physics & Astronomy, Louisiana State University, Baton Rouge, LA 70803, USA
[13] INAF Osservatorio Astronomico di Roma, Via Frascati 33, 00078 Monte Porzio Catone (RM), Italy
[14] Instituto de Astrofísica de Andalucía (CSIC), Apartado 3004, E–18080 Granada, Spain
[15] INAF—Osservatorio Astronomico di Brera, via E. Bianchi 46, I–23807 Merate, Italy
[16] Department of Physics and Astronomy, 20014 University of Turku, Finland
[17] Agenzia Spaziale Italiana, Via del Politecnico snc, 00133 Roma, Italy
[18] Physics Department and McDonnell Center for the Space Sciences, Washington University in St. Louis, St. Louis, MO 63130, USA
[19] Finnish Centre for Astronomy with ESO, University of Turku, 20014, Finland
[20] KIPAC and SLAC, Stanford University, Stanford, CA, 94305, USA
[21] Université de Strasbourg, CNRS, Observatoire Astronomique de Strasbourg, UMR 7550, 67000 Strasbourg, France
[22] Istituto Nazionale di Fisica Nucleare, Sezione di Torino, Via Pietro Giuria 1, 10125 Torino, Italy
[23] Dipartimento di Fisica, Universitá degli Studi di Torino, Via Pietro Giuria 1, 10125 Torino, Italy
[24] Department of Physical Sciences, Earth and Environment, Astronomical Observatory , University of Siena, Via Roma 56, 53100 Siena, Italy
[25] Department of Physics, University of Crete, 70013, Heraklion, Greece
[26] Institute of Astrophysics, Foundation for Research and Technology-Hellas, 71110 Heraklion, Greece
[27] Institute of Astrophysics, Voutes, 7110, Heraklion, Greece

[28] Crimean Astrophysical Observatory RAS, P/O Nauchny, 298409, Crimea[85]
[29] Special Astrophysical Observatory, Russian Academy of Sciences, 369167, Nizhnii Arkhyz, Russia
[30] Pulkovo Observatory, 196140 St. Petersburg, Russia
[31] Instituto de Astrofísica de Andalucía-CSIC, Glorieta de la Astronomía s/n, 18008, Granada, Spain
[32] Max Planck Institute for Radio Astronomy, Auf dem Huegel 69, Bonn, Germany
[33] Institut de Radioastronomie Millimétrique, Avenida Divina Pastora, 7, Local 20, E-18012 Granada, Spain
[34] Max-Planck-Institut für Radioastronomie, Auf dem Hügel 69, D-53121 Bonn, Germany
[35] Instituto de Astrofísicade Andalucía, IAA-CSIC, Glorieta de la Astronomía s/n, 18008 Granada, Spain
[36] Department of Physics, Graduate School of Advanced Science and Engineering, Hiroshima University Kagamiyama, 1-3-1 Higashi-Hiroshima, Hiroshima 739-8526, Japan
[37] Department of Physics, Tokyo Institute of Technology, 2-12-1 Ookayama, Meguro-ku, Tokyo 152-8551, Japan
[38] Hiroshima Astrophysical Science Center, Hiroshima University 1-3-1 Kagamiyama, Higashi-Hiroshima, Hiroshima 739-8526, Japan
[39] Core Research for Energetic Universe (Core-U), Hiroshima University, 1-3-1 Kagamiyama, Higashi-Hiroshima, Hiroshima 739-8526, Japan
[40] Planetary Exploration Research Center, Chiba Institute of Technology 2-17-1 Tsudanuma, Narashino, Chiba 275-0016, Japan
[41] California Institute of Technology, 1200 E. California Boulevard, Pasadena, CA 91125, USA
[42] University of California Santa Cruz, 1156 High Street, Santa Cruz, CA 95064, USA
[43] Graduate School of Sciences, Tohoku University, Aoba-ku, 980-8578 Sendai, Japan
[44] Astronomy Department, Boston University, 725 Commonwealth Avenue, Boston, MA 02215, USA
[45] Center for Astrophysics | Harvard & Smithsonian, 60 Garden Street, Cambridge, MA 02138, USA
[46] Korea Astronomy & Space Science Institute, Daedeokdae-ro 776,Yuseong-gu, Daejeon 34055, Republic of Korea
[47] University of Science and Technology, Gajeong-ro 217, Yuseong-gu, Daejeon 34113, Republic of Korea
[48] Section of Astrophysics, Astronomy & Mechanics, Department of Physics, National and Kapodistrian University of Athens, Panepistimiopolis Zografos 15784, Greece
[49] Joint ALMA Observatory, Alonso de Cordova 3107, Vitacura 763-0355, Santiago de Chile, Chile
[50] National Radio Astronomy Observatory, 520 Edgemont Road, Charlottesville, VA 22903-2475, USA
[51] Joint ALMA Observatory, Alonso de Cordova 3107 Vitacura, Santiago 763-0355, Chile
[52] NAOJ Chile Observatory, Alonso de Cordova 3788, Oficina 61B, Vitacura, Santiago, Chile
[53] European Southern Observatory, ESO Vitacura, Alonso de Cordova 3107, Vitacura, Casilla, 19001 Santiago, Chile
[54] Atacama Large Millimeter/submillimeter Array, ALMA Santiago Central Offices, Alonso de Cordova 3107, Vitacura, Casilla, 763-0355 Santiago, Chile
[55] National Astronomical Observatory of Japan, 2-21-1 Osawa, Mitaka, Tokyo 181-8588, Japan
[56] Department of Astronomical Science, The Graduate University for Advanced Studies (SOKENDAI), 2-21-1 Osawa, Mitaka, Tokyo 181-8588, Japan
[57] INAF Osservatorio Astronomico di Cagliari, Via della Scienza 5, 09047 Selargius (CA), Italy
[58] Istituto Nazionale di Fisica Nucleare, Sezione di Pisa, Largo B. Pontecorvo 3, 56127 Pisa, Italy
[59] Dipartimento di Fisica, Università di Pisa, Largo B. Pontecorvo 3, 56127 Pisa, Italy
[60] Dipartimento di Matematica e Fisica, Università degli Studi Roma Tre, Via della Vasca Navale 84, 00146 Roma, Italy
[61] Dipartimento di Fisica, Università degli Studi di Torino, Via Pietro Giuria 1, 10125 Torino, Italy
[62] INAF Osservatorio Astrofisico di Arcetri, Largo Enrico Fermi 5, 50125 Firenze, Italy
[63] Dipartimento di Fisica e Astronomia, Università degli Studi di Firenze, Via Sansone 1, 50019 Sesto Fiorentino (FI), Italy
[64] Istituto Nazionale di Fisica Nucleare, Sezione di Firenze, Via Sansone 1, 50019 Sesto Fiorentino (FI), Italy
[65] Space and Technology Institute, Universities Space Research Association, Huntsville, AL 35805, USA
[66] Istituto Nazionale di Fisica Nucleare, Sezione di Roma "Tor Vergata", Via della Ricerca Scientifica 1, 00133 Roma, Italy
[67] Institut für Astronomie und Astrophysik, Universität Tübingen, Sand 1, 72076 Tübingen, Germany
[68] Astronomical Institute of the Czech Academy of Sciences, Boční II 1401/1, 14100 Praha 4, Czech Republic
[69] RIKEN Cluster for Pioneering Research, 2-1 Hirosawa, Wako, Saitama 351-0198, Japan
[70] NASA Goddard Space Flight Center, Greenbelt, MD 20771, USA
[71] Yamagata University, 1-4-12 Kojirakawa-machi, Yamagata-shi 990-8560, Japan
[72] Osaka University, 1-1 Yamadaoka, Suita, Osaka 565-0871, Japan
[73] University of British Columbia, Vancouver, BC, V6T 1Z4, Canada
[74] International Center for Hadron Astrophysics, Chiba University, Chiba, 263-8522, Japan
[75] Department of Physics and Astronomy and Space Science Center, University of New Hampshire, Durham, NH 03824, USA
[76] Graduate School of Science, Division of Particle and Astrophysical Science, Nagoya University, Furo-cho, Chikusa-ku, Nagoya, Aichi 464-8602, Japan
[77] Department of Physics, The University of Hong Kong, Pokfulam, Hong Kong
[78] Department of Astronomy and Astrophysics, Pennsylvania State University, University Park, PA 16802, USA
[79] Université Grenoble Alpes, CNRS, IPAG, 38000 Grenoble, France
[80] Dipartimento di Fisica e Astronomia, Università degli Studi di Padova, Via Marzolo 8, 35131 Padova, Italy
[81] Department of Astronomy, University of Maryland, College Park, Maryland 20742, USA
[82] Mullard Space Science Laboratory, University College London, Holmbury St Mary, Dorking, Surrey, RH5 6NT, UK
[83] Anton Pannekoek Institute for Astronomy & GRAPPA, University of Amsterdam, Science Park 904, 1098 XH Amsterdam, The Netherlands
[84] Guangxi Key Laboratory for Relativistic Astrophysics, School of Physical Science and Technology, Guangxi University, Nanning 530004, People's Republic of China

Received 2023 October 5; revised 2024 May 27; accepted 2024 June 8; published 2024 August 26

Abstract

We present X-ray polarimetry observations from the Imaging X-ray Polarimetry Explorer (IXPE) of three low spectral peak and one intermediate spectral peak blazars, namely 3C 273, 3C 279, 3C 454.3, and S5 0716+714. For

[85] While the AAS journals adhere to and respect UN resolutions regarding the designations of territories (available at http://www.un.org/press/en), it is our policy to use the affiliations provided by our authors on published articles.

Original content from this work may be used under the terms of the Creative Commons Attribution 4.0 licence. Any further distribution of this work must maintain attribution to the author(s) and the title of the work, journal citation and DOI.

none of these objects was IXPE able to detect X-ray polarization at the 3σ level. However, we placed upper limits on the polarization degree at ∼10%–30%. The undetected polarizations favor models where the X-ray band is dominated by unpolarized photons upscattered by relativistic electrons in the jets of blazars, although hadronic models are not completely eliminated. We discuss the X-ray polarization upper limits in the context of our contemporaneous multiwavelength polarization campaigns.

Unified Astronomy Thesaurus concepts: X-ray astronomy (1810); Polarimetry (1278); Spectropolarimetry (1973); Radio loud quasars (1349); X-ray quasars (1821); Blazars (164); Flat-spectrum radio quasars (2163)

1. Introduction

Blazars are active galactic nuclei (AGNs) with relativistic jets that are inferred to be oriented within a few degrees from the observer's line of sight (see Blandford et al. 2019). Their spectral energy distributions (SEDs) are generally characterized by two emission components: one at low photon energies (radio through optical, UV, and, in some cases, X-ray bands) and the other at much higher (X-ray and γ-ray) energies. Blazars are often classified by the frequency at which the low-energy portion of the SED peaks. This component is modeled as electron synchrotron emission. When the peak frequency is below the optical or infrared (IR) band, the blazar is considered to be low synchrotron peaked (LSP), in contrast with high-synchrotron-peaked (HSP) blazars, whose peak is in the X-ray band. Objects with a peak in the optical/UV range are termed intermediate-synchrotron-peaked (ISP) blazars. The origin of the different synchrotron peak classes is still debated, but it is often attributed to increased particle cooling due to the presence of external photon fields (Fossati et al. 1998).

Several blazars were observed in 2022 with the Imaging X-ray Polarimetry Explorer (IXPE; Weisskopf et al. 2022) that was launched on 2021 December 9. HSP blazars such as Mrk 501 (Liodakis et al. 2022), Mrk 421 (Di Gesu et al. 2022a), and PG 1553+113 (Middei et al. 2023a) were measured by IXPE to be polarized in the 10%–15% range, 2–5 times higher than the optical polarization at the same epochs. These findings support a model by which the X-rays in HSPs are produced in energy-stratified shocks, with electrons accelerated at the shock front to energies high enough to emit X-ray synchrotron radiation. Such energetic electrons occur only in a thin layer close to the shock front, beyond which the maximum electron energy decreases owing to radiative cooling (Marscher & Gear 1985). Consequently, the optically emitting region, which requires somewhat lower electron energies, extends over a more extensive volume. If the magnetic field is mostly disordered, e.g., by turbulence, then the mean polarization variation is expected to be stronger due to the increased randomness of the polarization vectors of the emission regions (Di Gesu et al. 2022b). This could have a stronger effect on the X-ray emission regions, which should occupy a smaller volume of the jet (i.e., fewer emission zones) compared to the optical or radio regions. The ratio of X-ray to optical polarization was observed to be higher than expected in such a model, which suggests that the level of disorder of the magnetic field increases with distance from the shock front (Liodakis et al. 2022; Marscher & Jorstad 2022). The alignment of the electric vector position angle (EVPA) with the jet direction in Mrk 501 (Liodakis et al. 2022) implies that there is an ordered component to the magnetic field perpendicular to the jet. How this component arises is somewhat uncertain; various suggestions involve compression of the disordered field at the shock (Hughes et al. 1985), generation of a magnetic field component transverse to the shock normal (Tavecchio et al. 2018), or a toroidal magnetic field component in the ambient jet (Lyutikov et al. 2005). Complicating the physical picture of HSP blazar shocks are the observations that the EVPA can rotate in the X-ray band without rotation in the optical (Di Gesu et al. 2023) or vice versa (Middei et al. 2023a).

On the other hand, the X-ray portions of the SEDs of LSP and ISP blazars generally have flatter spectra than at optical frequencies (e.g., Abdo et al. 2010), indicating that a single synchrotron model is not responsible for both bands. The flatter X-ray spectra are consistent with models where the X-ray band is dominated by Compton upscattering of low-frequency (e.g., IR) photons by the relativistic electrons generating the synchrotron radiation (e.g., Maraschi et al. 2008). Processes involving hadrons, such as proton synchrotron radiation or production of electron–positron pairs by particle cascades might also be involved in generating the X-rays (e.g., Zhang et al. 2016). Each of these processes has specific polarization properties that can potentially identify their level of importance in the X-ray emission (e.g., Liodakis et al. 2019; Peirson et al. 2022). Compton scattering of unpolarized seed photons, such as those produced by the broad emission-line region, produces essentially unpolarized high-energy photons (Krawczynski 2012). If the seed photons are from synchrotron radiation in the jet—the synchrotron self-Compton (SSC) case—the X-ray polarization fraction (Π_X) is generally less than half that of the synchrotron radiation; the exact ratio depends on the model and the level of disorder of the magnetic field (Peirson et al. 2022). For hadronic processes, Π_X is expected to be similar to or even exceed the optical polarization (Π_O; Zhang & Böttcher 2013; Zhang et al. 2019). Hence, X-ray polarization measurements or even upper limits in the context of simultaneous multiwavelength polarization observations can test emission models for LSP and ISP blazars.

IXPE previously observed BL Lac on three occasions. In the first two observations, the X-ray spectrum of BL Lac resembled that of LSPs, in the third observation that of ISPs. During the first two observations, there was only a 99% confidence upper limit of $\Pi_X < 13\%$, while the contemporaneous Π_O exceeded the X-ray limits (Middei et al. 2023b). In the third observation, 22% polarization was detected in the 2–4 keV band during a time dominated by synchrotron-emitting electrons from the low-energy hump of the SED (Peirson et al. 2023). There are still only upper limits to the X-ray polarization from the high-energy component. Those results disfavor any significant contribution from protons to the emission.

In this study, we present results from IXPE observations of three LSP blazars and one ISP blazar that were observed in 2022: 3C 273, 3C 279, 3C 454.3, and S5 0716+714. In Section 2, we describe the IXPE observations with full-band polarimetric and spectropolarimetric analyses, in Section 3 we

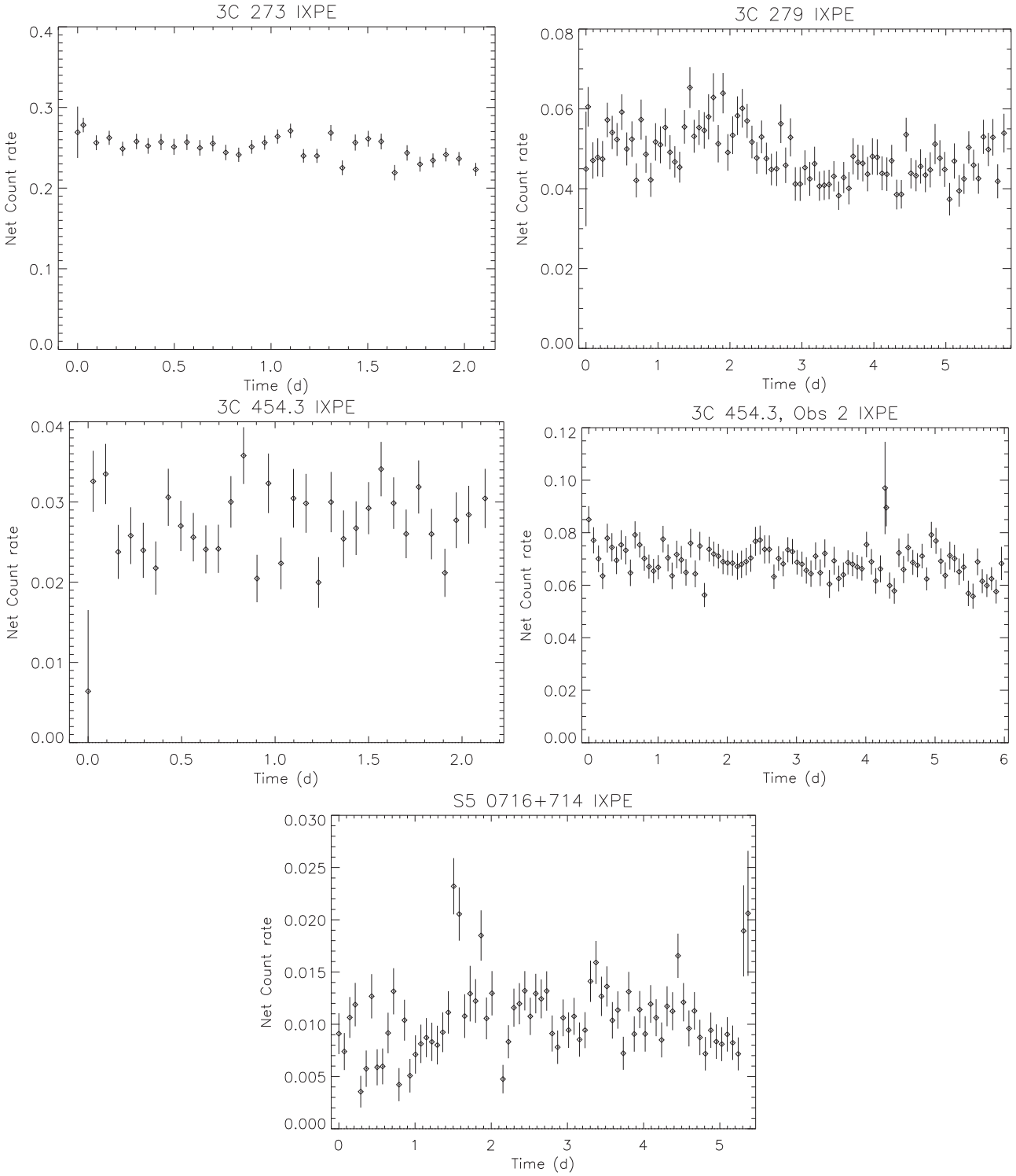

Figure 1. IXPE background-subtracted light curves for the four blazars reported here. No large variations are observed that would warrant isolating specific time periods for detailed analysis.

discuss the multiwavelength polarization campaigns on individual sources, and in Section 4 we discuss our results.

2. IXPE Observations

A log of IXPE observations is provided in Table 1. Two observations of 3C 454.3 were included, with the second one labeled "Obs 2." See Weisskopf et al. (2022) for details about IXPE. At the ∼30″ angular resolution of IXPE, all of these sources are spatially unresolved.

2.1. Full-band Analyses

Event data were selected over the full bandpass from 2 to 8 keV, from a circular region 60″ radius about each source, with background selected from an annulus from 200″ to 300″ from the target. Data were processed using `ixpeobssim`

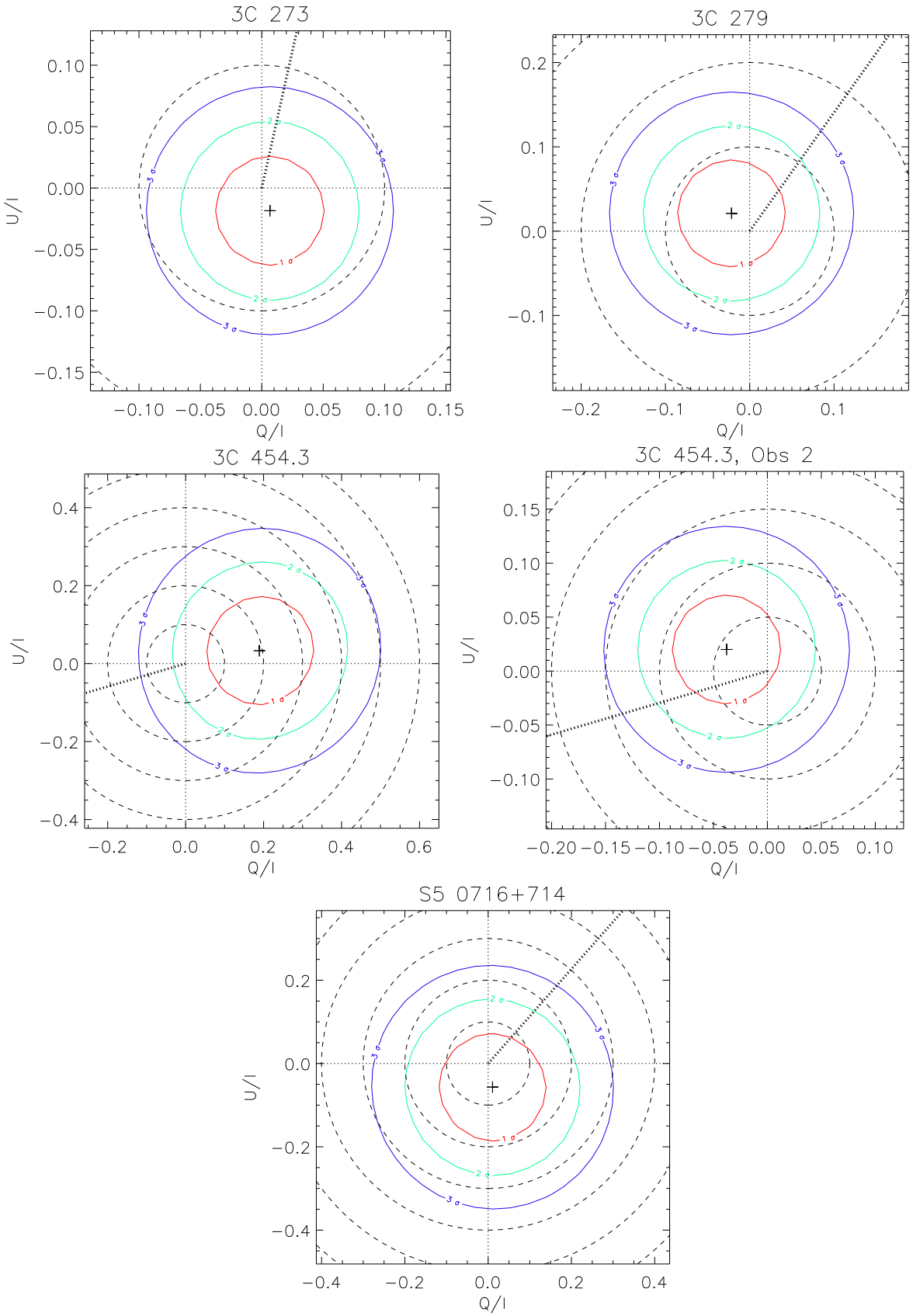

Figure 2. Probability contours in $Q-U$ space for time- and bandpass-averaged IXPE polarimetry of four blazars using a maximum-likelihood method that accounts for unpolarized background. Contour levels for 2 degrees of freedom enclose the 1σ, 2σ, and 3σ confidence regions. The plus signs mark the best estimates of $q = Q/I$ and $u = U/I$ and the dashed lines give circles of constant X-ray polarization fraction $\Pi_X = (q^2 + u^2)^{1/2}$ in 10% increments. The position angles of the jets are indicated by the thick dotted lines, taken from Weaver et al. (2019). In all cases, the results are consistent with null polarization at the 1–2σ confidence level.

Table 1
Summary of IXPE Observations

Source	Instrument	Observation ID	MJD Range	Exposure[a] (ks)	Π_X[b]
3C 273	IXPE	01005901	59732.37–59734.45	95.28	<9.0%
3C 279	IXPE	01005701	59743.02–59748.85	264.42	<12.7%
3C 454.3	IXPE	01005401	59730.19–59732.34	98.12	<28%
3C 454.3 (Obs 2)	IXPE	02008901	60115.92–60121.89	274.92	<10.1%
S5 0716+714	IXPE	01005301	59669.43–59674.80	358.68	<26%

Notes.
[a] Average of exposures for the three detector units.
[b] 99% confidence limits using the unbinned, event-based likelihood method (Section 2.1).

Table 2
Summary of Spectropolarimetric Results

Source	N_H (10^{20} cm^{-2})	Γ	K (10^{-3} ph cm^{-2} s^{-2} keV^{-1})	Π_X[a]
3C 273	1.68	1.80 ± 0.02	12.1	<12.8%
3C 279	2.25	1.79 ± 0.04	2.28	<15.5%
3C 454.3	6.81	1.71 ± 0.08	1.22	<40.3%
3C 454.3 (Obs 2)		1.66 ± 0.03	2.71	<11.6%
S5 0716+714	2.88	2.29 ± 0.20	0.72	<41.8%

Note.
[a] The 99% confidence upper limits on Π_X are computed using the Q and U best-fit Gaussian 1σ errors and the best-fit Q/I and U/I values. See Section 2.2 for details.

(Baldini et al. 2022) and standard `ftools` (provided by the NASA High Energy Astrophysics Science Archive Research Center 2014). Background-subtracted light curves are shown in Figure 1.

Results from an unbinned event-based likelihood analysis (Marshall 2021) that accounts for an unpolarized background (Marshall 2024) are shown in Figure 2. No clear detections of X-ray polarizations are observed at the 1–2σ confidence level, with 99% confidence limits ranging from 9% to 28% (Table 1).

Rotations of the EVPA during the IXPE observation, especially for exposures longer than the typical variability timescales (∼1–2 days) in blazars, can lead to depolarization, as was demonstrated recently in the X-ray EVPA rotation detected by IXPE in Mrk 421 (Di Gesu et al. 2023). We tested for rotations using the method described in Di Gesu et al. (2023), employing an event-based likelihood method (Marshall 2021). Briefly, event tracks are rotated according to a simple model where the EVPA rotates uniformly through the observation with rate ω (in degrees per day). The difference in the log-likelihood is $\Delta S = S(\omega; \hat{q}, \hat{u}) - S(0; \hat{q_0}, \hat{u_0})$, where $S(\omega; \hat{q}, \hat{u})$ is the log-likelihood at ω at the best-fit q and u for that value of ω. ΔS is distributed as χ^2 with 1 degree of freedom because q and u are uninteresting parameters for this test. We do not find evidence for EVPA rotations during our observations in any of the four sources. An example of the results from a rotation search is shown in Figure 3.

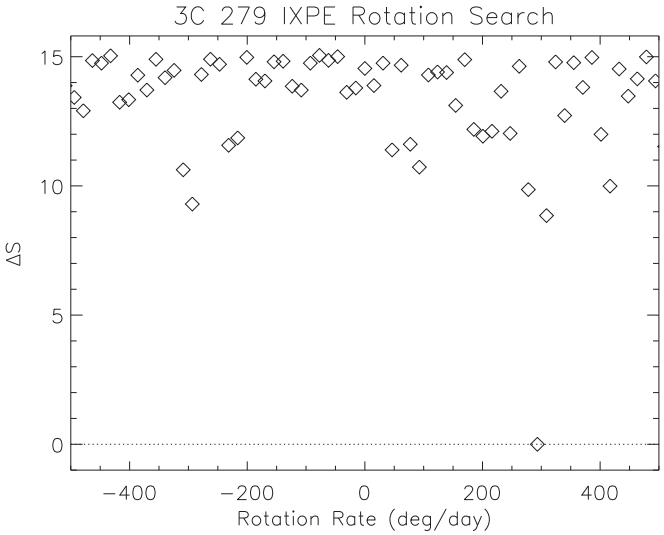

Figure 3. Example of a search for EVPA rotation, as applied to 3C 279. This source provided the largest log-likelihood difference of this group of blazars. A value of ΔS as large as 15.05 is significant at the 99.95% confidence level but there were about 130 trial rates tested, giving a chance detection of a rotation of this significance of 6.8%. See Di Gesu et al. (2023) for details of how the test was conducted.

2.2. Spectropolarimetry

Spectropolarimetric fits were performed with the Multi-Mission Maximum Likelihood (`3ML`) framework (Vianello et al. 2015).[86] In the 2–8 keV energy range, the spectra for the four sources are well described by an absorbed power law. The absorption column densities were fixed to the nominal Galactic values, and the polarization parameters are assumed to be constant through each observation and independent of energy.[87] Table 2 summarizes the best-fit parameters from the fits to each source, and Figure 4 shows the spectral fits. Figures 5 and 6 show the polarization parameters derived from the spectropolarimetric fits. An analysis using `xspec` gave similar results.

3. Notes on Individual Sources

Here we give information regarding the individual sources and our contemporaneous multiwavelength campaign during the IXPE observations. The results from the multiwavelength campaigns are summarized in the Appendix, and in Figures 7–11 and Tables 3–6.

[86] https://threeml.readthedocs.io/en/stable/index.html
[87] https://heasarc.gsfc.nasa.gov/cgi-bin/Tools/w3nh/w3nh.pl

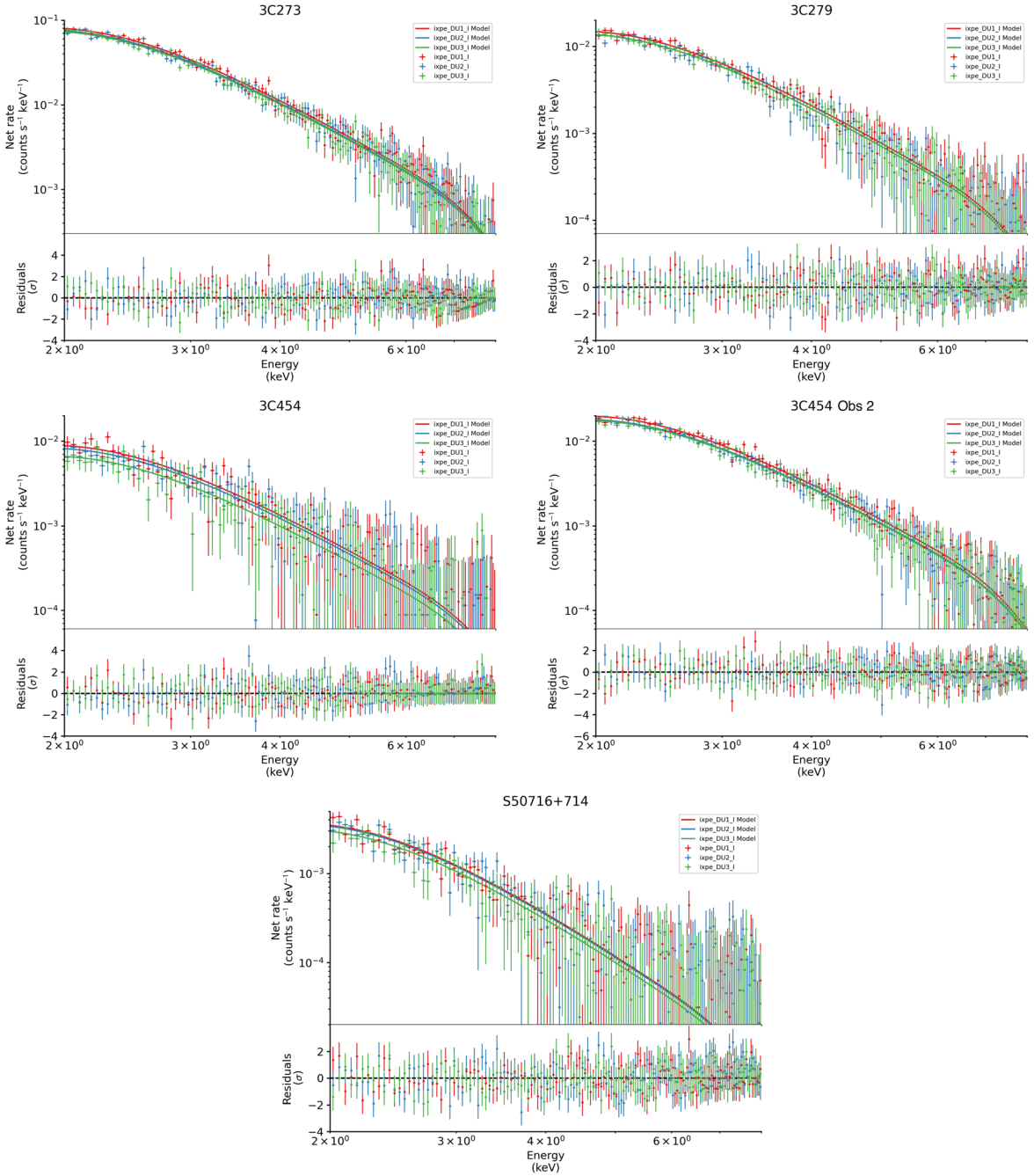

Figure 4. Background-subtracted Stokes *I* spectra for the four sources (from top left to bottom right: 3C 273, 3C 279, 3C 454.3, and S5 0716+714). In each plot, the solid lines show the best-fit model (absorbed power law), and the bottom panels illustrate the residuals of the data compared to the best-fit model. Red, blue, and green data and models represent IXPE DU1, DU2, and DU3, respectively.

3.1. 3C 273

3C273 ($z = 0.158339$) is one of the brightest X-ray-emitting LSP blazars. It is a flat-spectrum, radio-loud quasar with a strong "Big Blue Bump" that is interpreted as optical emission from an accretion disk (Shields 1978; Malkan 1983). Consistent with the interpretation that the optical light is of thermal origin, it is notoriously unpolarized (Stockman et al. 1984; Fernandes et al. 2020; Blinov et al. 2021b); hence, it is not surprising that the polarization in the *BVRI* bands was <0.5% during our contemporaneous optical/IR campaign. Complicating the interpretation of our results is that the X-ray emission in 3C 273 is most likely a mix of hot corona and jet emission (Grandi & Palumbo 2004; Chidiac et al. 2016). The nondetection (<9%) of X-ray polarization prevents us from discerning between these two possible origins of the X-ray emission.

3.2. 3C 279

3C 279 ($z = 0.538$) is one of the most rapidly varying blazars, showing minute-timescale variability in γ-rays (Ackermann et al. 2016). It is also known to show large optical EVPA variations (Kiehlmann et al. 2016) that might also be connected to repeating patterns of γ-ray activity (Blinov et al. 2021a). During the IXPE observation the source polarization

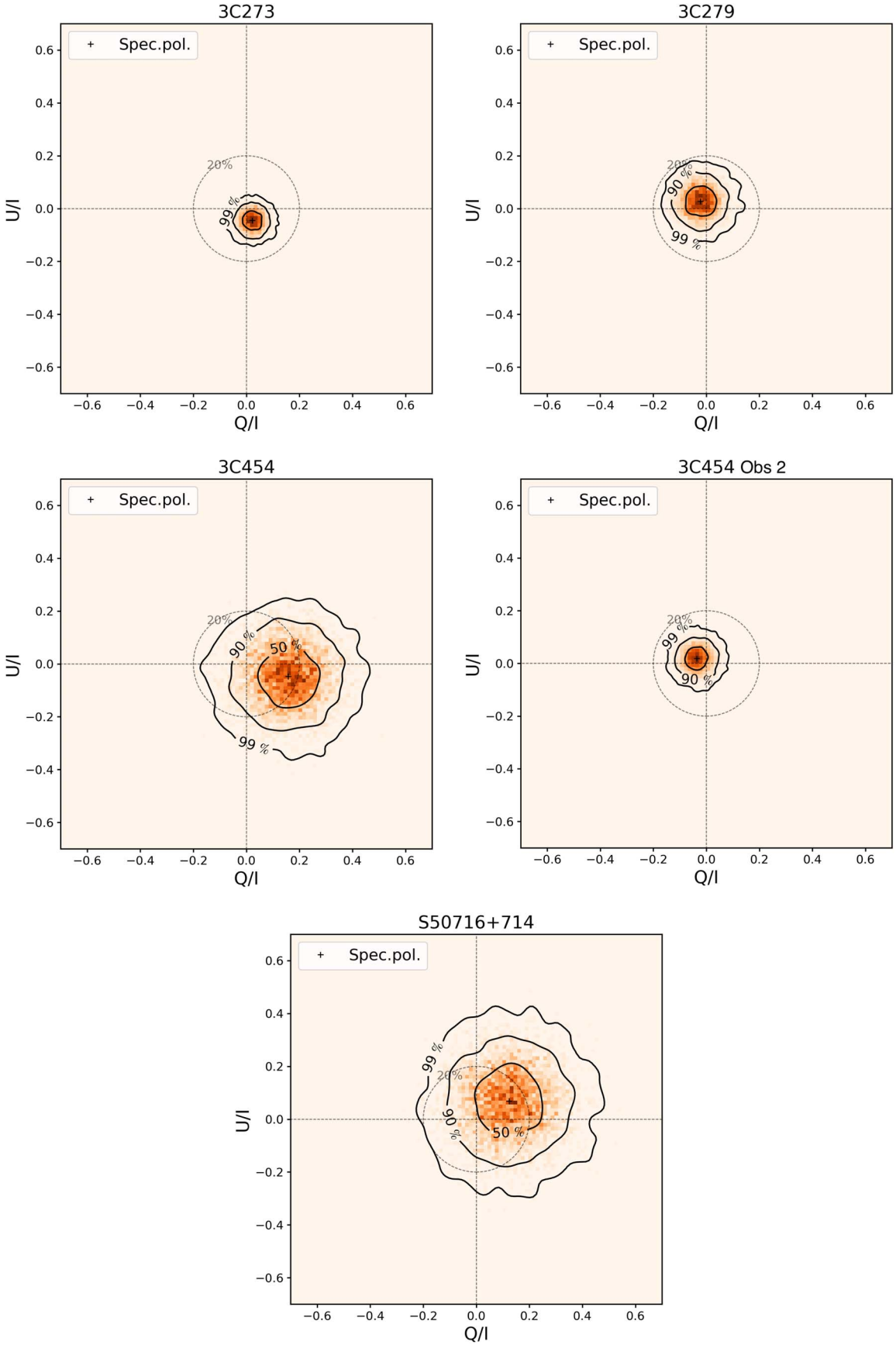

Figure 5. Stokes Q/I and U/I contour plots resulting from the spectropolarimetric fit for the four sources (from top left to bottom right: 3C 273, 3C 279, 3C 454.3, and S5 0716+714). Confidence levels of 50%, 90%, and 99% are shown, and the dotted circles indicate the locus where the polarization fraction is 20%.

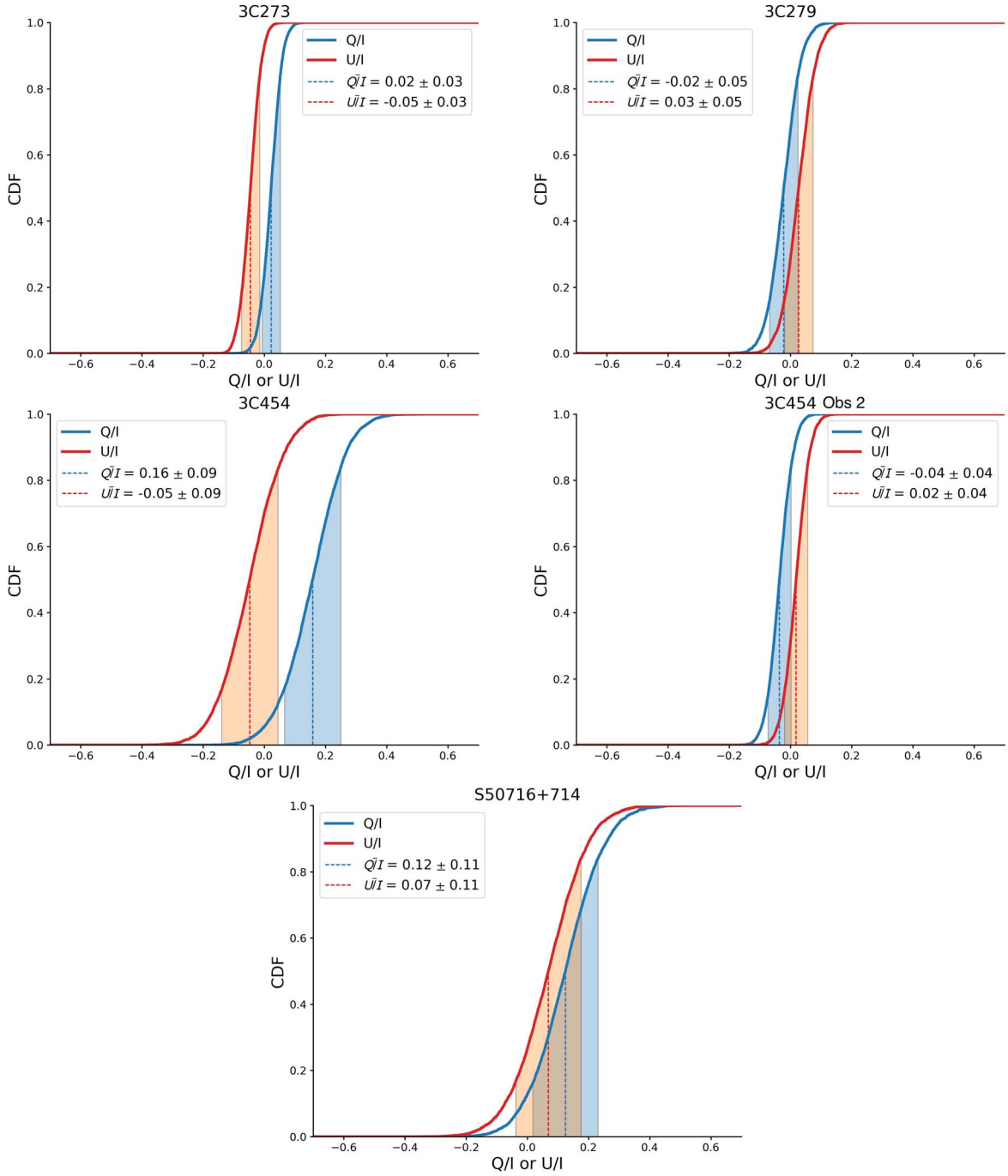

Figure 6. Stokes Q and U cumulative distribution functions (CDFs) for the best-fit distributions for the four sources (from top left to bottom right: 3C 273, 3C 279, 3C 454.3, and S5 0716+714).

was about 4% in millimeter (mm)–radio and 12% (within uncertainties) in optical/IR (*BVRIH*). The EVPA showed a mild decrease from ∼175° to ∼165° in the optical-IR bands. In a hadronic scenario, X-ray polarization should be stable—less variable than the optical polarization (Zhang et al. 2016). Given the low-amplitude, slow EVPA variability in the optical, and the fact we do not find evidence for significant variations of the X-ray EVPA (see Figure 3), we can exclude temporal depolarization effects. Thus, the fact that the optical/IR polarization degree is comparable to the X-ray upper limit (<12.7%) strongly disfavors models predicting higher X-ray polarization than the optical (e.g., proton synchrotron, proton-induced pair cascades, etc.).

3.3. 3C 454.3

3C 454.3 ($z = 0.859$) has had several well-studied outbursts observed across a wide swath of the electromagnetic spectrum (e.g., Jorstad et al. 2010, 2013; Weaver et al. 2019; Liodakis et al. 2020) and has exhibited peculiar jet behavior (e.g., disappearing jet components; Traianou et al. 2022). It showed large variation in the value of Π_O that can reach as high as 30% (Liodakis et al. 2020). We observed 3C 454.3 twice on 2022 May 31 until 2022 June 2 and again a year later 2023 June 20–2023 June 27. During the first IXPE observation (hereafter OBS1) the source was at best weakly polarized. In mm–radio, we obtain only upper limits of <0.8% at 3 mm and <3.3% at

1.3 mm. The optical (*VRI*) polarization is below 1%, with a stable EVPA within uncertainties. During the second IXPE observation (hereafter OBS2) we observe a slightly higher polarization degree that reaches a peak of 2%. The polarization angle is fairly stable, consistent with OBS1, until the end of the IXPE observation. There we observe a rapid rotation, likely related to the drop of Π_O. At the end of the IXPE observation Π_O drops below detectable levels (<0.3%). After the IXPE observation, the angle recovers as Π_O slightly increases. In the mm–radio, the source shows a stable polarization angle consistent with the optical observations, and slightly higher polarization degree at around 2%–3%. Lower-frequency radio observations (<86 GHz) with the Korean VLBI Network (KVN) and Monitoring the Stokes *Q*, *U*, *I* and *V* Emission of AGN jets in Radio (QUIVER) programs (see Table 5) showed consistent results. That might suggest that the optical emission during our IXPE observations came from highly turbulent regions, which would explain the atypical for the source low Π_O. The unpolarized state in the optical in combination with the X-ray upper limits (<28% and <10.1%) prevents us from coming to any conclusion regarding the emission processes in this source, but it may be interesting to reobserve this target when Π_O is much higher.

3.4. S5 0716+714

S5 0716+714 ($z = 0.3$) is a highly variable source that often shows intra-night variability in multiple optical bands (e.g., Gupta et al. 2012), large outbursts across the electromagnetic spectrum, and TeV emission (e.g., MAGIC Collaboration et al. 2018). During the IXPE observation, the source was observed in several optical and IR bands (*BVRIJHK*) showing highly variable Π_O between 1% and 13%. There is a large change in the optical EVPA before the IXPE observations (from ∼125° to ∼50°). During the observation, we observe a slow optical EVPA increase from ∼50° to ∼100°. Unfortunately, the source was in a quiescent X-ray flux state, providing an upper limit to the X-ray polarization of <26%. Given the level of optical/IR polarization, we can only exclude models that predict several factors higher X-ray polarization than optical. We note that the X-ray spectral index is steeper for this source than the others presented here, perhaps an indication of its ISP nature that might provide a more significant X-ray polarization detection during a soft X-ray flare.

4. Summary

We presented results from the first-year observations of LSP and ISP sources by IXPE, namely 3C 273, 3C 279, 3C 454.3, and S5 0716+714. All the IXPE observations were supplemented with a contemporaneous radio/optical/IR polarization campaign. None of the sources yielded a significant ($>3\sigma$) X-ray polarization detection. Instead, we are able to constrain Π_X in the 2–8 keV band to be <13% for 3C 273 and 3C 279 and <28% for 3C 454.3 and S5 0716+714. The nondetection of X-ray polarization in these sources is consistent with previous IXPE results on BL Lac in both LSP and ISP states (Middei et al. 2023b; Peirson et al. 2023) as well as other radio galaxies (Ehlert et al. 2022).

For 3C 273 and 3C 454.3, the undetected X-ray polarization could point toward Compton scattering, either external Compton or SSC; however, the unpolarized optical/IR emission during the IXPE observations is preventing us from coming to definitive conclusions. For S5 0716+714, the highly variable optical polarization degree and the high upper limit (<26%) on the X-ray polarization makes any interpretation difficult. Our results disfavor a scenario where the X-ray polarization is a factor of several higher than the optical. Such a scenario can involve, for example, a pure proton synchrotron model (Zhang & Böttcher 2013; Paliya et al. 2018; Zhang et al. 2019) or scattering from relativistically moving plasma containing relatively cold electrons (Begelman & Sikora 1987).

On the other hand, 3C 279 shows fairly stable Π and EVPA in the optical/IR that remains persistently high (>10%) and an upper limit to the Π_X that is comparable (<12.7%). IXPE observations of BL Lac showed a similar picture, i.e., undetected X-ray polarization (<16%) with Π_O that is comparable or exceeds the X-ray limits (Middei et al. 2023b; Peirson et al. 2023). However, in the case of BL Lac, the highly variable EVPA we observe in the optical could lead to depolarization of the otherwise highly polarized proton synchrotron emission, making it consistent with the Π_X limits. In the case of 3C 279, we can exclude any such depolarization effects, therefore our results strongly disfavor a significant contribution from proton synchrotron to the emission. While our results cannot yet differentiate between scattering or other hadronic processes, the emerging pattern of IXPE LSP/ISP observations suggests that $\Pi_X \lesssim 10\%$ and less than or comparable to the contemporaneous Π_O. Further IXPE observations can help further elucidate the X-ray emission mechanism in LSP/ISP blazars.

Acknowledgments

The IXPE is a joint US and Italian mission. The US contribution is supported by the National Aeronautics and Space Administration (NASA) and led and managed by its Marshall Space Flight Center (MSFC), with industry partner Ball Aerospace (contract NNM15AA18C). The Italian contribution is supported by the Italian Space Agency (Agenzia Spaziale Italiana, ASI) through contract ASI-OHBI-2017-12-I.0, agreements ASI-INAF-2017-12-H0 and ASI-INFN-2017.13-H0, and its Space Science Data Center (SSDC) with agreements ASI-INAF-2022-14-HH.0 and ASI-INFN 2021-43-HH.0, and by the Istituto Nazionale di Astrofisica (INAF) and the Istituto Nazionale di Fisica Nucleare (INFN) in Italy. This research used data products provided by the IXPE Team (MSFC, SSDC, INAF, and INFN) and distributed with additional software tools by the High-Energy Astrophysics Science Archive Research Center (HEASARC), at NASA Goddard Space Flight Center (GSFC). Funding for this work was provided in part by contract 80MSFC17C0012 from the MSFC to MIT in support of the IXPE project. Support for this work was provided in part by the National Aeronautics and Space Administration (NASA) through the Smithsonian Astrophysical Observatory (SAO) contract SV3-73016 to MIT for support of the Chandra X-ray Center (CXC), which is operated by SAO for and on behalf of NASA under contract NAS8-03060. I.L and B.A.-G. were funded by the European Union ERC-2022-STG—BOOTES—101076343. The views and opinions expressed are, however, those of the author(s) only and do not necessarily reflect those of the European Union or the European Research Council Executive Agency. Neither the European Union nor the granting authority can be held responsible for them. This research has made use of data from the RoboPol program, a collaboration between Caltech, the

University of Crete, IA-FORTH, IUCAA, the MPIfR, and the Nicolaus Copernicus University, which was conducted at Skinakas Observatory in Crete, Greece. The IAA-CSIC coauthors acknowledge financial support from the Spanish "Ministerio de Ciencia e Innovacion" (MCINN) through the "Center of Excellence Severo Ochoa" award for the Instituto de Astrofísica de Andalucía-CSIC (SEV-2017-0709). Acquisition and reduction of the POLAMI, TOP-MAPCAR, and OSN data was supported in part by MICINN through grant Nos. AYA2016-80889-P and PID2019-107847RB-C44. Some of the data are based on observations collected at the Observatorio de Sierra Nevada, owned and operated by the Instituto de Astrofísica de Andalucía (IAA-CSIC). Further data are based on observations collected at the Centro Astronómico Hispano-Alemán (CAHA), operated jointly by Junta de Andalucía and Consejo Superior de Investigaciones Científicas (IAA-CSIC). The POLAMI observations were carried out at the IRAM 30 m Telescope. IRAM is supported by INSU/CNRS (France), MPG (Germany), and IGN (Spain). Some of the data reported here are based on observations obtained at the Hale Telescope, Palomar Observatory as part of a continuing collaboration between the California Institute of Technology, NASA/JPL, Yale University, and the National Astronomical Observatories of China. G.V.P. acknowledges support by NASA through the NASA Hubble Fellowship grant No. HST-HF2-51444.001-A awarded by the Space Telescope Science Institute, which is operated by the Association of Universities for Research in Astronomy, Inc., under NASA contract NAS5-26555. The data in this study include observations made with the Nordic Optical Telescope, owned in collaboration by the University of Turku and Aarhus University, and operated jointly by Aarhus University, the University of Turku and the University of Oslo, representing Denmark, Finland, and Norway, the University of Iceland and Stockholm University at the Observatorio del Roque de los Muchachos, La Palma, Spain, of the Instituto de Astrofisica de Canarias. The data presented here were obtained in part with ALFOSC, which is provided by the Instituto de Astrofísica de Andalucía (IAA) under a joint agreement with the University of Copenhagen and NOT. E.L. was supported by Academy of Finland projects 317636 and 320045. D.B., S.K., R.S., and N.M. acknowledge support from the European Research Council (ERC) under the European Unions Horizon 2020 research and innovation program under grant agreement No. 771282. C.C. acknowledges support by the European Research Council (ERC) under the HORIZON ERC Grants 2021 program under grant agreement No. 101040021. The Dipol-2 polarimeter was built in cooperation by the University of Turku, Finland, and the Leibniz Institut für Sonnenphysik, Germany, with support from the Leibniz Association grant No. SAW-2011-KIS-7. This work was supported by JST, the establishment of university fellowships toward the creation of science technology innovation, grant No. JPMJFS2129. This work was supported by the Japan Society for the Promotion of Science (JSPS) KAKENHI grant No. JP21H01137. This work was also partially supported by the Optical and Near-Infrared Astronomy Inter-University Cooperation Program from the Ministry of Education, Culture, Sports, Science and Technology (MEXT) of Japan. We are grateful to the observation and operating members of Kanata Telescope. The research at Boston University was supported in part by National Science Foundation grant AST-2108622, NASA Fermi Guest Investigator grant No. 80NSSC23K1507, and NASA Swift Guest Investigator grant No. 80NSSC22K0537. This study used observations conducted with the 1.8 m Perkins Telescope Observatory (PTO) in Arizona (USA), which is owned and operated by Boston University. The Submillimeter Array is a joint project between the Smithsonian Astrophysical Observatory and the Academia Sinica Institute of Astronomy and Astrophysics and is funded by the Smithsonian Institution and the Academia Sinica. Maunakea, the location of the SMA, is a culturally important site for the indigenous Hawaiian people; we are privileged to study the cosmos from its summit. The KVN is a facility operated by the Korea Astronomy and Space Science Institute. The KVN operations are supported by Korea Research Environment Open NETwork (KREONET), which is managed and operated by the Korea Institute of Science and Technology Information (KISTI). Partly based on observations with the 100 m telescope of the Max-Planck-Institut für Radioastronomie (MPIfR) at Effelsberg. Observations with the 100 m radio telescope at Effelsberg have received funding from the European Union's Horizon 2020 research and innovation program under grant agreement No. 101004719 (ORP). This paper makes use of the following ALMA director's discretionary time data under proposal ESO#2021.A.00016.T. ALMA is a partnership of ESO (representing its member states), NSF (USA), and NINS (Japan), together with NRC (Canada), MOST and ASIAA (Taiwan), and KASI (Republic of Korea), in cooperation with the Republic of Chile. The Joint ALMA Observatory is operated by ESO, AUI/NRAO and NAOJ.

Facilities: ALMA, CAO:2.2m, CrAO:0.7m, Effelsberg, IRAM:30m, IXPE, LX-200, Kanata, KVN, NOT, Hale, Perkins, Skinakas:1.3m, SMA, Swift, TU:0.6m (DIPOL-2).

Software: ixpeobssim (Baldini et al. 2022), Astropy (Astropy Collaboration et al. 2013, 2018), Photutils (Bradley et al. 2019), NumPy and SciPy (Virtanen et al. 2020), IPython (Perez & Granger 2007), HEASoft 6.30.1[88] (NASA High Energy Astrophysics Science Archive Research Center 2014), `3ML` (Vianello et al. 2015).

Appendix
Multiwavelength Polarization Observations

Contemporaneous to the IXPE observations, several telescopes across the world provided multiwavelength polarization observations from radio to optical. Not all participating telescopes were able to observe all sources and in all listed radio frequencies and optical bands. Below we list the participating telescopes with a short description. Details on the different telescopes, analysis pipelines, and observing strategy can be found in Liodakis et al. (2022), Di Gesu et al. (2022b, 2023), and Kim et al. (2024). Tables 3–6 list the median values for the polarization degree and EVPA during the IXPE observations for the individual radio and optical telescopes. Figures 7–11 show the optical observations for the individual sources. Since our radio observations are limited in comparison to the optical results, and often only yield upper limits, we have opted to not include them in the plots to improve visibility. In the mm–radio spectral bands, observations were obtained with the IRAM 30 m telescope as part of the Polarimetric Monitoring of AGN at Millimeter Wavelengths (POLAMI[89]) project at 3.5 mm (86.24 GHz) and 1.3 mm (228.93 GHz; Agudo et al.

[88] http://heasarc.gsfc.nasa.gov/ftools
[89] http://polami.iaa.es/

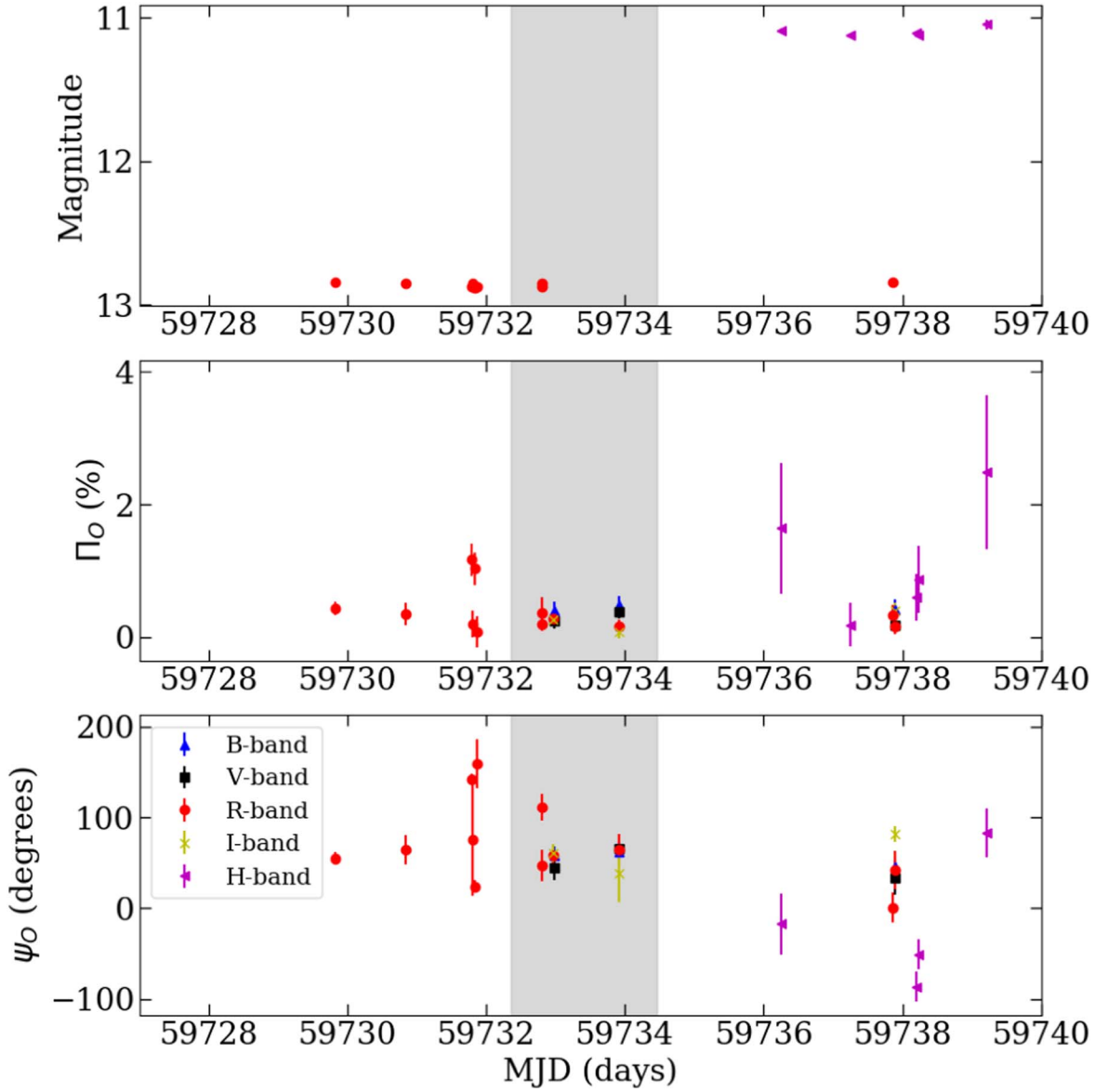

Figure 7. Contemporaneous optical and IR observations of 3C 273. The top panel shows the brightness in magnitudes, the middle panel the polarization degree, and the bottom panel the EVPA. The gray shaded area marks the duration of the IXPE observation.

2018a, 2018b; Thum et al. 2018), the Submillimeter Array (SMA) taken at 225.5 GHz within the SMA Monitoring of AGNs with Polarization (SMAPOL) program (I. Myserlis et al. 2024, in preparation) using two orthogonally polarized receivers, the SMA polarimeter, and standard analysis and calibration procedures (Sault et al. 1995; Ho et al. 2004; Marrone & Rao 2008; Primiani et al. 2016). Additional observations were obtained with the Atacama Large Millimeter Array (ALMA[90]) at 343.5 GHz. Lower-frequency radio observations were obtained through the KVN (22–86 GHz; Kang et al. 2015) and QUIVER program (4.85–17 GHz) using the Effelsberg 100 m telescope. Observations in the *J*, *H*, and *K* IR bands were obtained using the 200 inch Palomar Hale telescope and the WIRC+Pol[91] instrument (Tinyanont et al. 2019a, 2019b; Millar-Blanchaer et al. 2021; Masiero et al. 2022), the Kanata telescope using the Hiroshima Optical and Near-InfraRed camera (HONIR; Kawabata et al. 1999; Akitaya et al. 2014), and the IR camera MIMIR[92] (Clemens et al. 2012) at the Perkins Telescope (PTO; Flagstaff, AZ). In the optical, observations in the *B*, *V*, *R*, and *I* bands were obtained by the AZT-8 and LX-200 telescopes (St. Petersburg University), the Calar Alto and Sierra Nevada observatories, the DIPOL-2 polarimeter at the Haleakala observatory T60 telescope (Piirola 1973; Kosenkov et al. 2017; Berdyugin et al. 2018, 2019; Piirola et al. 2021), HONIR at the Kanata telescope, the Alhambra Faint Object Spectrograph and Camera (ALFOSC) at the Nordic Optical Telescope (NOT. Hovatta et al. 2016; Nilsson et al. 2018), and the RoboPol polarimeters at the Skinakas observatory (Panopoulou et al. 2015; Ramaprakash et al. 2019; Blinov et al. 2021b).

[90] https://www.alma.cl/skameno/AMAPOLA/
[91] https://github.com/WIRC-Pol/wirc_drp
[92] https://people.bu.edu/clemens/mimir/index.html

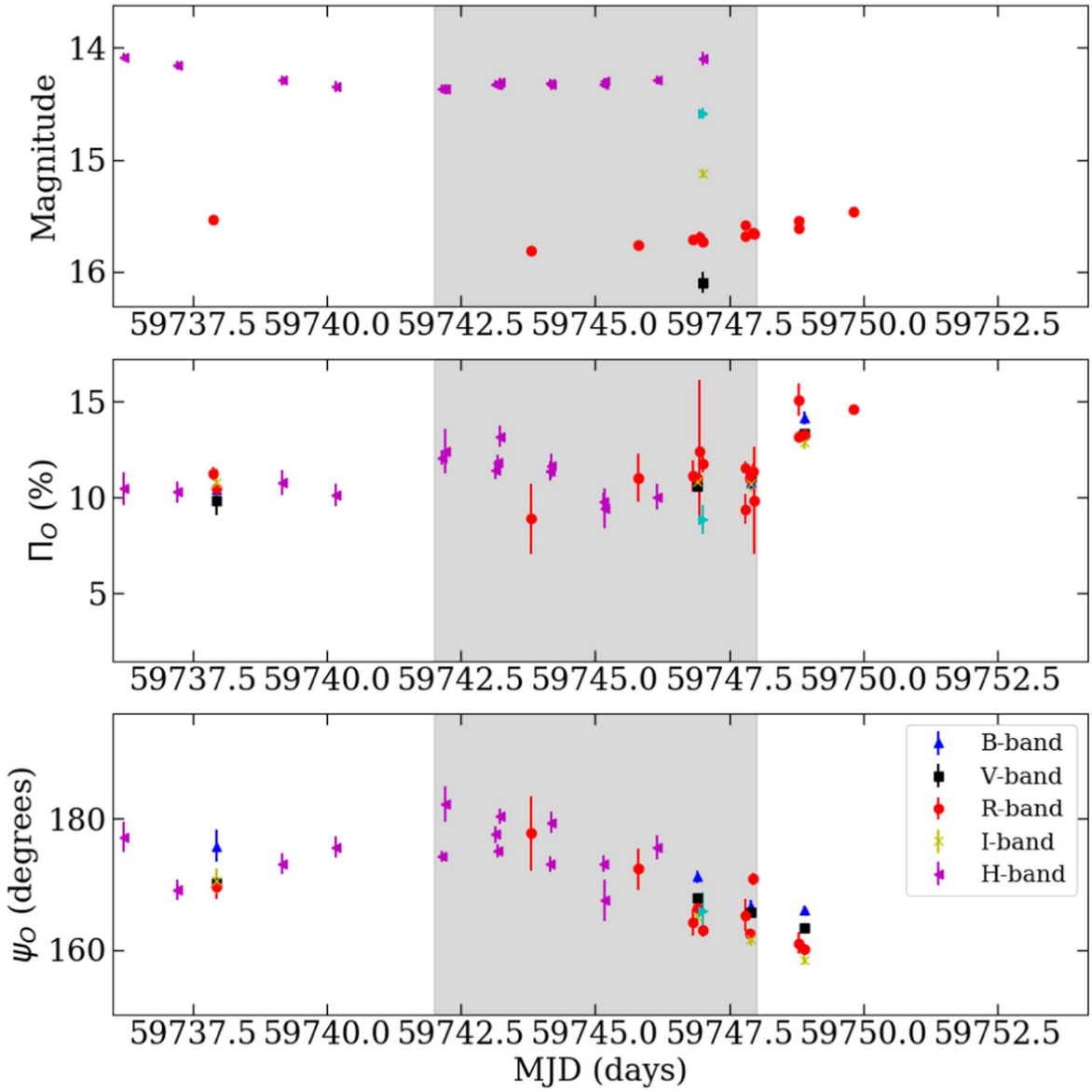

Figure 8. Same as Figure 7 but for 3C 279.

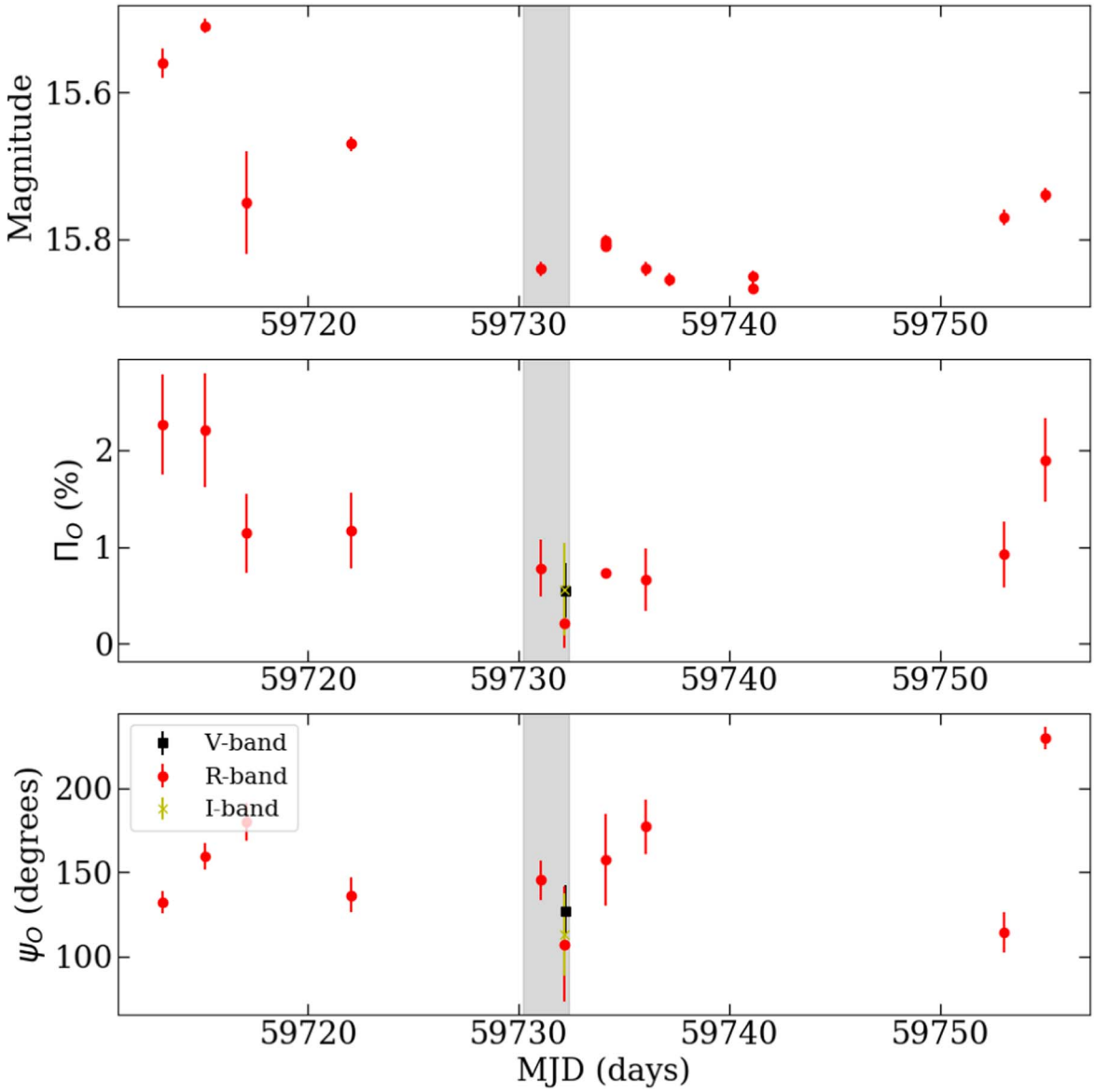

Figure 9. Same as Figure 7 but for 3C 454.3 (OBS1).

Table 3
Polarization Results Contemporaneous with the IXPE Observation of 3C 273

Telescope	Π (%)	s_Π	ψ (deg)	s_ψ
POLAMI (3 mm)	5.55 ± 1.17	0.06	146 ± 6	0.3
POLAMI (1.3 mm)	5.23 ± 0.8	0.58	150 ± 4	6.6
SMA (225.5 GHz)	5.63 ± 0.8	⋯	130 ± 0.2	⋯
AZT-8 and LX-200 (*R* band)	0.38 ± 0.23	⋯	111 ± 14	⋯
NOT (*B* band)	0.45 ± 0.13	0.05	60 ± 9	1.45
NOT (*V* band)	0.31 ± 0.11	0.07	55 ± 11	10.5
NOT (*R* band)	0.23 ± 0.1	0.05	61 ± 14	3.4
NOT (*I* band)	0.18 ± 0.1	0.09	50 ± 21	11.1
Skinakas (*R* band)	0.2 ± 0.1	⋯	47 ± 17	⋯

Note. The uncertainties for Π and ψ (i.e., EVPA) are either the uncertainty of the measurement or the median uncertainty in the case of multiple measurements. The quantities s_Π and s_ψ represent the standard deviations of Π or ψ, respectively.

Table 4
Polarization Results Contemporaneous with the IXPE Observation of 3C 279

Telescope	Π (%)	s_Π	ψ (deg)	s_ψ
POLAMI (3 mm)	4.09 ± 0.34	0.15	179 ± 2	0.84
POLAMI (1.3 mm)	<4.6	⋯	⋯	⋯
SMA (225.5 GHz)	4.08 ± 0.56	⋯	172 ± 1	⋯
AZT-8 and LX-200 (*R* band)	10.2 ± 1	0.97	169 ± 3	5.5
Calar Alto and SNO (*R* band)	11 ± 2	3.4	154 ± 6	10.6
Kanata (*R* band)	11.75 ± 0.42	⋯	163 ± 1	⋯
Kanata (*J* band)	8.88 ± 0.75	⋯	166 ± 3	⋯
NOT (*B* band)	10.77 ± 0.35	0.03	169 ± 1	2.26
NOT (*V* band)	10.86 ± 0.26	0.23	167 ± 0.7	1.1
NOT (*R* band)	11.01 ± 0.26	0.01	164.4 ± 0.6	2.04
NOT (*I* band)	10.79 ± 0.36	0.07	163.3 ± 1	1.72
Perkins (*H* band)	11.54 ± 0.5	1.13	175 ± 1	4.06
Skinakas (*R* band)	11.55 ± 0.33	⋯	160.4 ± 0.8	⋯

Note. See the Table 3 note.

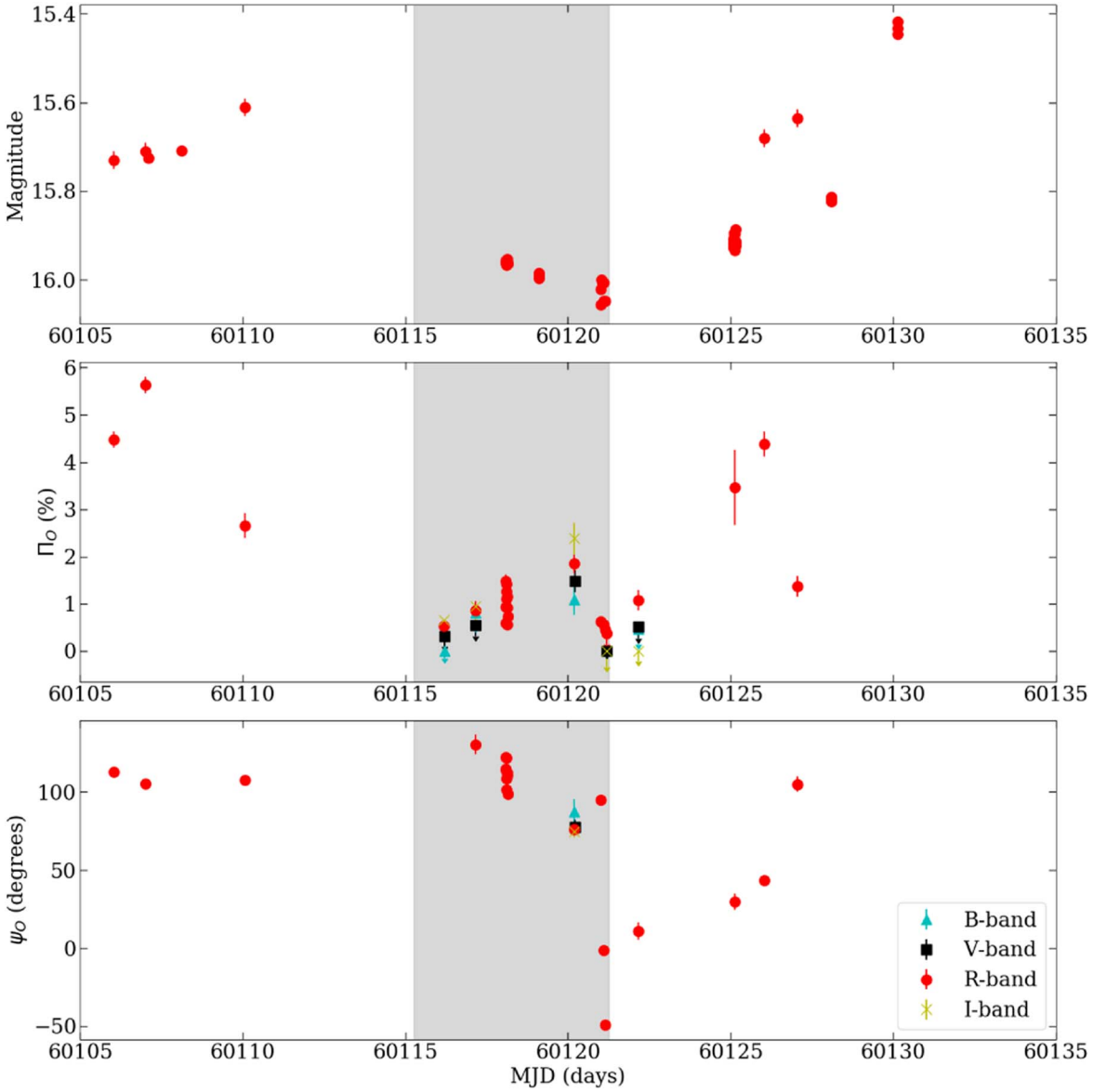

Figure 10. Same as Figure 7 but for 3C 454.3 (OBS2).

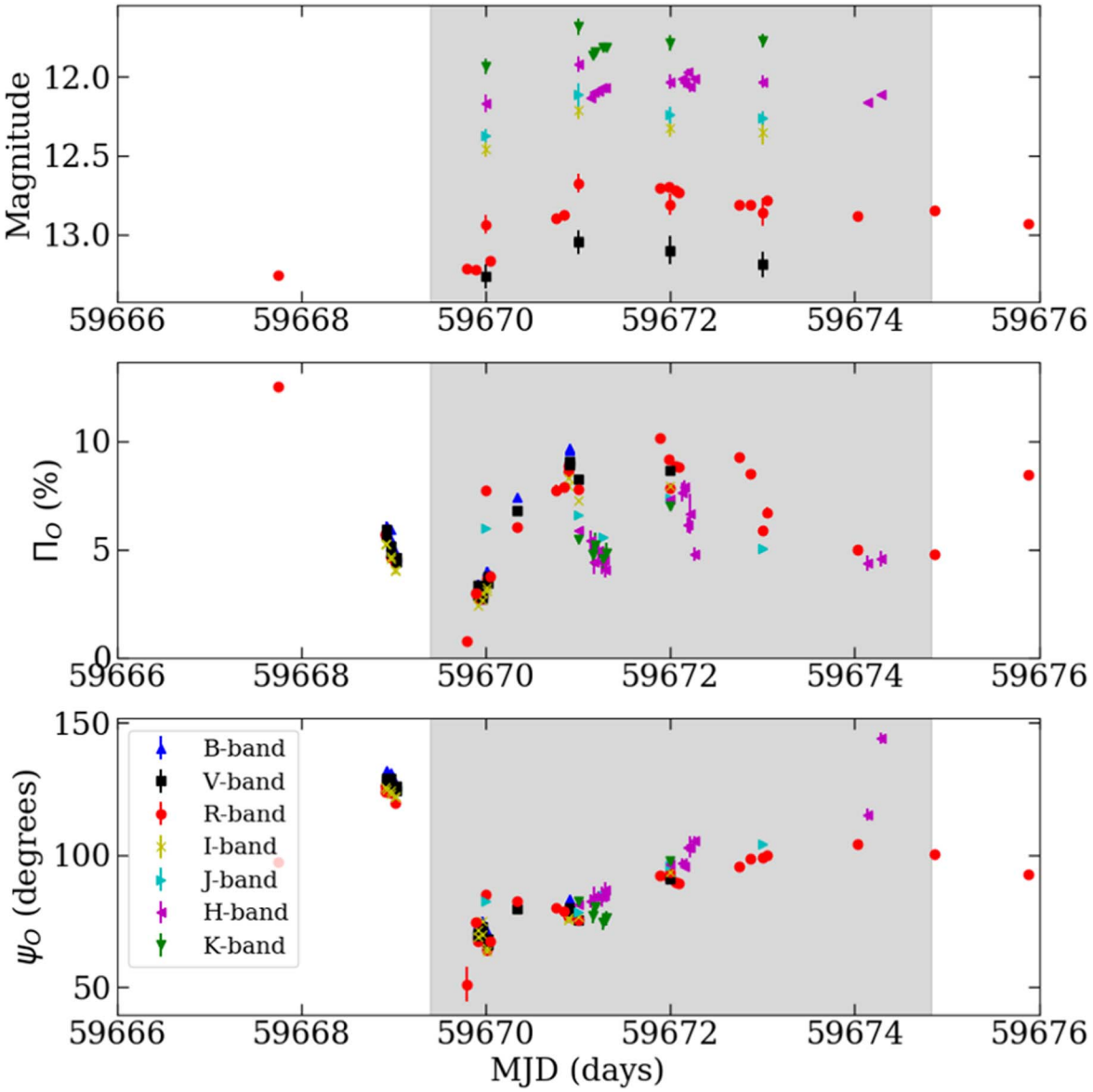

Figure 11. Same as Figure 7 but for S5 0716+714.

Table 5
Polarization Results Contemporaneous with the IXPE Observation of 3C 454.3

Telescope	Π (%)	s_Π	ψ (deg)	s_ψ
OBS1				
KVN (22 GHz)	0.46 ± 0.09	⋯	92 ± 3	⋯
KVN (43 GHz)	0.65 ± 0.09	⋯	121 ± 8	⋯
KVN (86 GHz)	1.3 ± 0.4	⋯	120 ± 12	⋯
KVN (129 GHz)	<3.4	⋯	⋯	⋯
POLAMI (3 mm)	<0.82	⋯	⋯	⋯
POLAMI (1.3 mm)	<3.3	⋯	⋯	⋯
SMA (225.5 GHz)	2.1 ± 0.3	⋯	112 ± 2	⋯
AZT-8 and LX-200 (*R* band)	<1	⋯	⋯	⋯
Calar Alto (*R* band)	0.72 ± 0.3	0.28	157 ± 15	27
NOT (*B* band)	<1	⋯	⋯	⋯
NOT (*V* band)	0.55 ± 0.3	⋯	127 ± 15	⋯
NOT (*R* band)	0.21 ± 0.25	⋯	107 ± 34	⋯
NOT (*I* band)	0.56 ± 0.48	⋯	113 ± 25	⋯
Skinakas (*R* band)	0.67 ± 0.33	⋯	145 ± 12	⋯
OBS2				
ALMA (343.5 GHz)	2.58 ± 0.3	⋯	133 ± 2	⋯
KVN (22 GHz)	2.0 ± 0.08	⋯	106 ± 3	⋯
KVN (43 GHz)	2.1 ± 0.09	⋯	105 ± 2	⋯
KVN (86 GHz)	2.6 ± 0.3	⋯	111 ± 3	⋯
SMA (225.5 GHz)	2.5 ± 0.3	0.55	130 ± 0.7	2.41
Calar Alto (*R* band)	0.9 ± 0.3	0.33	110 ± 4	50
NOT (*B* band)	0.4 ± 0.2	0.48	88 ± 8	⋯
NOT (*V* band)	0.43 ± 0.2	0.55	77 ± 5	⋯
NOT (*R* band)	0.7 ± 0.2	0.57	103 ± 5	27
NOT (*I* band)	0.80 ± 0.3	0.86	75 ± 4	⋯

Note. See the Table 3 note.

Table 6
Polarization Results Contemporaneous with the IXPE Observation of S5 0716+714

Telescope	Π (%)	s_Π	ψ (deg)	s_ψ
POLAMI (3 mm)	<1.1	⋯	⋯	⋯
POLAMI (1.3 mm)	<3.8	⋯	⋯	⋯
AZT-8 and LX-200 (*R* band)	7.86 ± 0.17	2.76	89.7 ± 0.6	14.24
Kanata (*R* band)	7.75 ± 0.04	0.83	89.2 ± 0.13	9.01
Kanata (*J* band)	6.28 ± 0.06	0.84	89.4 ± 0.2	10.24
NOT (*B* band)	3.59 ± 0.18	2.74	74 ± 1.4	5.05
NOT (*V* band)	3.39 ± 0.14	2.53	71.2 ± 1.3	4.54
NOT (*R* band)	3.19 ± 0.14	2.47	69 ± 1.2	4.57
NOT (*I* band)	3.03 ± 0.13	2.28	71 ± 1.2	4.41
Palomar (*J* band)	4.52 ± 0.07	⋯	85 ± 1	⋯
Palomar (*H* band)	5.57 ± 0.07	0	85 ± 1	⋯
Perkins (*H* band)	4.86 ± 0.38	1.26	96 ± 2.2	16.95
Perkins (*K* band)	4.81 ± 0.49	0.22	77 ± 2.9	2.25
T60 (*B* band)	7.41 ± 0.12	⋯	82.1 ± 0.5	⋯
T60 (*V* band)	6.8 ± 0.16	⋯	79.8 ± 0.7	⋯
T60 (*R* band)	6.04 ± 0.15	⋯	82.8 ± 0.7	⋯

Note. See the Table 3 note.

ORCID iDs

Herman L. Marshall https://orcid.org/0000-0002-6492-1293
Ioannis Liodakis https://orcid.org/0000-0001-9200-4006
Alan P. Marscher https://orcid.org/0000-0001-7396-3332
Niccolò Di Lalla https://orcid.org/0000-0002-7574-1298
Svetlana G. Jorstad https://orcid.org/0000-0001-6158-1708
Dawoon E. Kim https://orcid.org/0000-0001-5717-3736
Riccardo Middei https://orcid.org/0000-0001-9815-9092
Michela Negro https://orcid.org/0000-0002-6548-5622
Nicola Omodei https://orcid.org/0000-0002-5448-7577
Abel L. Peirson https://orcid.org/0000-0001-6292-1911
Matteo Perri https://orcid.org/0000-0003-3613-4409
Simonetta Puccetti https://orcid.org/0000-0002-2734-7835
Marco Laurenti https://orcid.org/0000-0001-5762-6360
Iván Agudo https://orcid.org/0000-0002-3777-6182
Giacomo Bonnoli https://orcid.org/0000-0003-2464-9077
Andrei V. Berdyugin https://orcid.org/0000-0002-9353-5164
Elisabetta Cavazzuti https://orcid.org/0000-0001-7150-9638
Nicole Rodriguez Cavero https://orcid.org/0000-0001-5256-0278
Immacolata Donnarumma https://orcid.org/0000-0002-4700-4549
Laura Di Gesu https://orcid.org/0000-0002-5614-5028
Henric Krawczynski https://orcid.org/0000-0002-1084-6507
Frédéric Marin https://orcid.org/0000-0003-4952-0835
Francesco Massaro https://orcid.org/0000-0002-1704-9850
Luigi Pacciani https://orcid.org/0000-0001-6897-5996
Juri Poutanen https://orcid.org/0000-0002-0983-0049
Fabrizio Tavecchio https://orcid.org/0000-0003-0256-0995
Beatriz Agís-González https://orcid.org/0000-0001-7702-8931
César Husillos https://orcid.org/0000-0001-8286-5443
Alessandro Marchini https://orcid.org/0000-0003-3779-6762
Alfredo Sota https://orcid.org/0000-0002-9404-6952
Ioakeim G. Bourbah https://orcid.org/0000-0002-8597-6154
Raphael Skalidis https://orcid.org/0000-0003-2337-0277
George A. Borman https://orcid.org/0000-0002-7262-6710
Evgenia N. Kopatskaya https://orcid.org/0000-0001-9518-337X
Elena G. Larionova https://orcid.org/0000-0002-2471-6500
Daria A. Morozova https://orcid.org/0000-0002-9407-7804
Sergey S. Savchenko https://orcid.org/0000-0003-4147-3851
Andrey A. Vasilyev https://orcid.org/0000-0002-8293-0214
Carolina Casadio https://orcid.org/0000-0003-1117-2863
Juan Escudero https://orcid.org/0000-0002-4131-655X
Joana Kramer https://orcid.org/0009-0003-3011-0454
Ioannis Myserlis https://orcid.org/0000-0003-3025-9497
Ryo Imazawa https://orcid.org/0000-0002-0643-7946
Yasushi Fukazawa https://orcid.org/0000-0002-0921-8837
Makoto Uemura https://orcid.org/0000-0002-7375-7405

Tsunefumi Mizuno https://orcid.org/0000-0001-7263-0296
Hiroshi Akitaya https://orcid.org/0000-0001-6156-238X
Joseph R. Masiero https://orcid.org/0000-0003-2638-720X
Dimitri Mawet https://orcid.org/0000-0002-8895-4735
Georgia V. Panopoulou https://orcid.org/0000-0001-7482-5759
Mark Gurwell https://orcid.org/0000-0003-0685-3621
Garrett Keating https://orcid.org/0000-0002-3490-146X
Sincheol Kang https://orcid.org/0000-0002-0112-4836
Sang-Hyun Kim https://orcid.org/0000-0001-7556-8504
Sang-Sung Lee https://orcid.org/0000-0002-6269-594X
Seiji Kameno https://orcid.org/0000-0002-5158-0063
Hiroshi Nagai https://orcid.org/0000-0003-0292-3645
Lucio A. Antonelli https://orcid.org/0000-0002-5037-9034
Matteo Bachetti https://orcid.org/0000-0002-4576-9337
Luca Baldini https://orcid.org/0000-0002-9785-7726
Wayne H. Baumgartner https://orcid.org/0000-0002-5106-0463
Ronaldo Bellazzini https://orcid.org/0000-0002-2469-7063
Stefano Bianchi https://orcid.org/0000-0002-4622-4240
Stephen D. Bongiorno https://orcid.org/0000-0002-0901-2097
Raffaella Bonino https://orcid.org/0000-0002-4264-1215
Alessandro Brez https://orcid.org/0000-0002-9460-1821
Niccolò Bucciantini https://orcid.org/0000-0002-8848-1392
Fiamma Capitanio https://orcid.org/0000-0002-6384-3027
Simone Castellano https://orcid.org/0000-0003-1111-4292
Chen-Ting Chen https://orcid.org/0000-0002-4945-5079
Stefano Ciprini https://orcid.org/0000-0002-0712-2479
Enrico Costa https://orcid.org/0000-0003-4925-8523
Alessandra De Rosa https://orcid.org/0000-0001-5668-6863
Ettore Del Monte https://orcid.org/0000-0002-3013-6334
Alessandro Di Marco https://orcid.org/0000-0003-0331-3259
Victor Doroshenko https://orcid.org/0000-0001-8162-1105
Michal Dovčiak https://orcid.org/0000-0003-0079-1239
Steven R. Ehlert https://orcid.org/0000-0003-4420-2838
Teruaki Enoto https://orcid.org/0000-0003-1244-3100
Yuri Evangelista https://orcid.org/0000-0001-6096-6710
Sergio Fabiani https://orcid.org/0000-0003-1533-0283
Riccardo Ferrazzoli https://orcid.org/0000-0003-1074-8605
Javier A. Garcia https://orcid.org/0000-0003-3828-2448
Shuichi Gunji https://orcid.org/0000-0002-5881-2445
Jeremy Heyl https://orcid.org/0000-0001-9739-367X
Wataru Iwakiri https://orcid.org/0000-0002-0207-9010
Philip Kaaret https://orcid.org/0000-0002-3638-0637
Vladimir Karas https://orcid.org/0000-0002-5760-0459
Fabian Kislat https://orcid.org/0000-0001-7477-0380
Jeffery J. Kolodziejczak https://orcid.org/0000-0002-0110-6136
Fabio La Monaca https://orcid.org/0000-0001-8916-4156
Luca Latronico https://orcid.org/0000-0002-0984-1856
Simone Maldera https://orcid.org/0000-0002-0698-4421
Alberto Manfreda https://orcid.org/0000-0002-0998-4953
Andrea Marinucci https://orcid.org/0000-0002-2055-4946
Giorgio Matt https://orcid.org/0000-0002-2152-0916
Fabio Muleri https://orcid.org/0000-0003-3331-3794
C.-Y. Ng https://orcid.org/0000-0002-5847-2612
Stephen L. O'Dell https://orcid.org/0000-0002-1868-8056
Chiara Oppedisano https://orcid.org/0000-0001-6194-4601
Alessandro Papitto https://orcid.org/0000-0001-6289-7413
George G. Pavlov https://orcid.org/0000-0002-7481-5259
Melissa Pesce-Rollins https://orcid.org/0000-0003-1790-8018
Pierre-Olivier Petrucci https://orcid.org/0000-0001-6061-3480
Maura Pilia https://orcid.org/0000-0001-7397-8091
Andrea Possenti https://orcid.org/0000-0001-5902-3731
Brian D. Ramsey https://orcid.org/0000-0003-1548-1524
John Rankin https://orcid.org/0000-0002-9774-0560
Ajay Ratheesh https://orcid.org/0000-0003-0411-4243
Oliver J. Roberts https://orcid.org/0000-0002-7150-9061
Roger W. Romani https://orcid.org/0000-0001-6711-3286
Carmelo Sgrò https://orcid.org/0000-0001-5676-6214
Patrick Slane https://orcid.org/0000-0002-6986-6756
Paolo Soffitta https://orcid.org/0000-0001-8916-4156
Gloria Spandre https://orcid.org/0000-0003-0802-3453
Douglas A. Swartz https://orcid.org/0000-0002-2954-4461
Toru Tamagawa https://orcid.org/0000-0002-8801-6263
Roberto Taverna https://orcid.org/0000-0002-1768-618X
Allyn F. Tennant https://orcid.org/0000-0002-9443-6774
Nicholas E. Thomas https://orcid.org/0000-0003-0411-4606
Francesco Tombesi https://orcid.org/0000-0002-6562-8654
Alessio Trois https://orcid.org/0000-0002-3180-6002
Sergey S. Tsygankov https://orcid.org/0000-0002-9679-0793
Roberto Turolla https://orcid.org/0000-0003-3977-8760
Jacco Vink https://orcid.org/0000-0002-4708-4219
Martin C. Weisskopf https://orcid.org/0000-0002-5270-4240
Kinwah Wu https://orcid.org/0000-0002-7568-8765
Fei Xie https://orcid.org/0000-0002-0105-5826
Silvia Zane https://orcid.org/0000-0001-5326-880X

References

Abdo, A. A., Ackermann, M., Agudo, I., et al. 2010, ApJ, 716, 30
Ackermann, M., Anantua, R., Asano, K., et al. 2016, ApJL, 824, L20
Agudo, I., Thum, C., Molina, S. N., et al. 2018a, MNRAS, 474, 1427
Agudo, I., Thum, C., Ramakrishnan, V., et al. 2018b, MNRAS, 473, 1850
Akitaya, H., Moritani, Y., Ui, T., et al. 2014, Proc. SPIE, 9147, 91474O
Astropy Collaboration, Price-Whelan, A. M., Sipőcz, B. M., et al. 2018, AJ, 156, 123
Astropy Collaboration, Robitaille, T. P., Tollerud, J. E., et al. 2013, A&A, 558, A33
Baldini, L., Bucciantini, N., Lalla, N. D., et al. 2022, SoftX, 19, 101194
Begelman, M. C., & Sikora, M. 1987, ApJ, 322, 650
Berdyugin, A., Piirola, V., & Poutanen, J. 2019, in Astronomical Polarization from the Infrared to Gamma Rays, ed. R. Mignani et al., Vol. 460 (Cham: Springer), 33
Berdyugin, A. V., Berdyugina, S. V., & Piirola, V. 2018, Proc. SPIE, 10702, 107024Z
Blandford, R., Meier, D., & Readhead, A. 2019, ARA&A, 57, 467
Blinov, D., Jorstad, S. G., Larionov, V. M., et al. 2021a, MNRAS, 505, 4616
Blinov, D., Kiehlmann, S., Pavlidou, V., et al. 2021b, MNRAS, 501, 3715
Bradley, L., Sipőcz, B., Robitaille, T., et al. 2019, astropy/photutils: v0.7.2, Zenodo, doi:10.5281/zenodo.3568287
Chidiac, C., Rani, B., Krichbaum, T. P., et al. 2016, A&A, 590, A61
Clemens, D. P., Pinnick, A. F., & Pavel, M. D. 2012, ApJS, 200, 20
Di Gesu, L., Donnarumma, I., Tavecchio, F., et al. 2022a, ApJL, 938, L7
Di Gesu, L., Marshall, H. L., Ehlert, S. R., et al. 2023, NatAs, 7, 1245
Di Gesu, L., Tavecchio, F., Donnarumma, I., et al. 2022b, A&A, 662, A83
Ehlert, S. R., Ferrazzoli, R., Marinucci, A., et al. 2022, ApJ, 935, 116
Fernandes, S., Patiño-Álvarez, V. M., Chavushyan, V., Schlegel, E. M., & Valdés, J. R. 2020, MNRAS, 497, 2066
Fossati, G., Maraschi, L., Celotti, A., Comastri, A., & Ghisellini, G. 1998, MNRAS, 299, 433

Grandi, P., & Palumbo, G. G. C. 2004, Sci, 306, 998
Gupta, A. C., Krichbaum, T. P., Wiita, P. J., et al. 2012, MNRAS, 425, 1357
Ho, P. T. P., Moran, J. M., & Lo, K. Y. 2004, ApJL, 616, L1
Hovatta, T., Lindfors, E., Blinov, D., et al. 2016, A&A, 596, A78
Hughes, P. A., Aller, H. D., & Aller, M. F. 1985, ApJ, 298, 301
Jorstad, S. G., Marscher, A. P., Larionov, V. M., et al. 2010, ApJ, 715, 362
Jorstad, S. G., Marscher, A. P., Smith, P. S., et al. 2013, ApJ, 773, 147
Kang, S., Lee, S.-S., & Byun, D.-Y. 2015, JKAS, 48, 257
Kawabata, K. S., Okazaki, A., Akitaya, H., et al. 1999, PASP, 111, 898
Kiehlmann, S., Savolainen, T., Jorstad, S. G., et al. 2016, A&A, 592, C1
Kim, D. E., Di Gesu, L., Liodakis, I., et al. 2024, A&A, 681, A12
Kosenkov, I. A., Berdyugin, A. V., Piirola, V., et al. 2017, MNRAS, 468, 4362
Krawczynski, H. 2012, ApJ, 744, 30
Liodakis, I., Blinov, D., Jorstad, S. G., et al. 2020, ApJ, 902, 61
Liodakis, I., Marscher, A. P., Agudo, I., et al. 2022, Natur, 611, 677
Liodakis, I., Peirson, A. L., & Romani, R. W. 2019, ApJ, 880, 29
Lyutikov, M., Pariev, V. I., & Gabuzda, D. C. 2005, MNRAS, 360, 869
MAGIC Collaboration, Ahnen, M. L., Ansoldi, S., et al. 2018, A&A, 619, A45
Malkan, M. A. 1983, ApJ, 268, 582
Maraschi, L., Foschini, L., Ghisellini, G., Tavecchio, F., & Sambruna, R. M. 2008, MNRAS, 391, 1981
Marrone, D. P., & Rao, R. 2008, Proc. SPIE, 7020, 70202B
Marscher, A. P., & Jorstad, S. G. 2022, Univ, 8, 644
Marscher, A. P., & Gear, W. K. 1985, ApJ, 298, 114
Marshall, H. L. 2021, ApJ, 907, 82
Marshall, H. L. 2024, ApJ, 964, 88
Masiero, J. R., Tinyanont, S., & Millar-Blanchaer, M. A. 2022, PSJ, 3, 90
Middei, R., Liodakis, I., Perri, M., et al. 2023b, ApJL, 942, L10
Middei, R., Perri, M., Puccetti, S., et al. 2023a, ApJL, 953, L28
Millar-Blanchaer, M. A., Tinyanont, S., Jovanovic, N., et al. 2021, Proc. SPIE, 11447, 1315
NASA High Energy Astrophysics Science Archive Research Center 2014, HEAsoft: Unified Release of FTOOLS and XANADU, Astrophysics Source Code Library, ascl:1408.004
Nilsson, K., Lindfors, E., Takalo, L. O., et al. 2018, A&A, 620, A185
Paliya, V. S., Zhang, H., Böttcher, M., et al. 2018, ApJ, 863, 98
Panopoulou, G., Tassis, K., Blinov, D., et al. 2015, MNRAS, 452, 715
Peirson, A. L., Liodakis, I., & Romani, R. W. 2022, ApJ, 931, 59
Peirson, A. L., Negro, M., Liodakis, I., et al. 2023, ApJL, 948, L25
Perez, F., & Granger, B. E. 2007, CSE, 9, 21
Piirola, V. 1973, A&A, 27, 383
Piirola, V., Kosenkov, I. A., Berdyugin, A. V., Berdyugina, S. V., & Poutanen, J. 2021, AJ, 161, 20
Primiani, R. A., Young, K. H., Young, A., et al. 2016, JAI, 5, 1641006
Ramaprakash, A. N., Rajarshi, C. V., Das, H. K., et al. 2019, MNRAS, 485, 2355
Sault, R. J., Teuben, P. J., & Wright, M. C. H. 1995, in ASP Conf. Ser. 77, Astronomical Data Analysis Software and Systems IV, ed. R. A. Shaw, H. E. Payne, & J. J. E. Hayes (San Francisco, CA: ASP), 433
Shields, G. A. 1978, Natur, 272, 706
Stockman, H. S., Moore, R. L., & Angel, J. R. P. 1984, ApJ, 279, 485
Tavecchio, F., Landoni, M., Sironi, L., & Coppi, P. 2018, MNRAS, 480, 2872
Thum, C., Agudo, I., Molina, S. N., et al. 2018, MNRAS, 473, 2506
Tinyanont, S., Millar-Blanchaer, M., Jovanovic, N., et al. 2019a, Proc. SPIE, 11132, 1113209
Tinyanont, S., Millar-Blanchaer, M. A., Nilsson, R., et al. 2019b, PASP, 131, 025001
Traianou, E., Krichbaum, T., Gomez, J. L., et al. 2022, in COSPAR Scientific Assembly 44, 2037
Vianello, G., Lauer, R. J., Younk, P., et al. 2015, arXiv:1507.08343
Virtanen, P., Gommers, R., Oliphant, T. E., et al. 2020, NatMe, 17, 261
Weaver, Z. R., Balonek, T. J., Jorstad, S. G., et al. 2019, ApJ, 875, 15
Weisskopf, M. C., Soffitta, P., Baldini, L., et al. 2022, JATIS, 8, 026002
Zhang, H., & Böttcher, M. 2013, ApJ, 774, 18
Zhang, H., Diltz, C., & Böttcher, M. 2016, ApJ, 829, 69
Zhang, H., Fang, K., Li, H., et al. 2019, ApJ, 876, 109